

UNCLASSIFIED

AD NUMBER
AD383325
NEW LIMITATION CHANGE
TO Approved for public release, distribution unlimited
FROM Distribution: Further dissemination only as directed by Aerospace Research Labs., Office of Aerospace Research, USAF, WPAFB, Ohio; Apr 1967 or higher DoD authority.
AUTHORITY
AFAL LTR 17 SEP 1979

THIS PAGE IS UNCLASSIFIED

UNCLASSIFIED

AD 383325-6

FROM CONFIDENTIAL
TO UNCLASSIFIED

PER AUTHORITY ARL, USAF ITR.

DATE 28 Feb. 72

DEFENSE DOCUMENTATION CENTER
CAMERON STATION
ALEXANDRIA, VIRGINIA 22314

UNCLASSIFIED

CONFIDENTIAL

ARL 67-0065

APRIL 1967



Aerospace Research Laboratories

AD 383325

THRUST AUGMENTATION FOR V/STOL: ARL's Research and Concepts (U)

AUG 24 1967

CAPT. WILLIAM S. CAMPBELL

DR. HANS VON OHAIN

OFFICE OF AEROSPACE RESEARCH
United States Air Force



CONFIDENTIAL

ARL 67-0065

CONFIDENTIAL

THRUST AUGMENTATION FOR V/STOL:
ARL'S RESEARCH AND CONCEPTS

WILLIAM S. CAMPBELL
HANS VON OHAIN
ENERGETICS RESEARCH LABORATORY

APRIL 1967

PROJECT 7116

STATEMENT #5 CLASSIFIED

In addition to the information contained in this document
and marked as such, the information is to be controlled by the holder only
with specific reference to ATTN (ARIR)

AEROSPACE RESEARCH LABORATORIES
OFFICE OF AEROSPACE RESEARCH
UNITED STATES AIR FORCE
WRIGHT-PATTERSON AIR FORCE BASE, OHIO

AFLC-W PAFB-AUG 67 354

CONFIDENTIAL

FOREWORD

The authors wish to thank Dr. Roscoe H. Mills for his contributions and stimulating discussions which significantly helped to crystallize ARL's thrust augmentation concepts, and Colonel Robert E. Fontana for his help in the initial phases of the project. Also, we wish to express our appreciation to Colonel Paul G. Atkinson, Jr., and Colonel Charles A. Scolatti. Their early recognition of the technological significance of advanced thrust augmentation for V/STOL and other aerospace propulsion applications led to their management decision to greatly strengthen ARL's in-house effort and to involve, at the earliest possible date, other Government and industrial organizations.

This report, with many revisions and additions, is the final form of the authors' preliminary technical report: "Jet Wing V/STOL Aircraft Employing Thrust Augmentation", ARL 67-0011, January 1967.

ABSTRACT

This report deals with the Aerospace Research Laboratories' (ARL) efforts in achieving thrust augmentation for air-breathing propulsion systems. Qualitative and quantitative analyses of the thrust augmentation process are reported and compared with experimental results. Application of the process to V/STOL propulsion is also discussed.

TABLE OF CONTENTS

SECTION	PAGE
I. INTRODUCTION	1
II. THRUST AUGMENTATION PROCESSES	2
III. PERFORMANCE ANALYSIS OF THRUST AUGMENTATION PROCESSES	6
IV. ARL'S TEST APPARATUS AND TEST RESULTS	8
V. THRUST AUGMENTATION — V/STOL COMPATIBILITY	10
VI. LONG-RANGE FUNDAMENTAL AND ENGINEERING RESEARCH	13

LIST OF FIGURES

Figure Number		Page
1.	Fluid Dynamic Energy Transfer	15
2.	Definitions and Relations in Thrust Augmentation Processes	16
3.	Multi-Dimensional Flow Effects	17
4.	Straight Flow Ejectors	18
5.	Main Losses in Thrust Augmentation Processes	19
6.	Velocity Versus Pressure Ratio for Gases of Different Sonic Speeds	20
7.	Gas-Gas Energy Transfer	21
8.	Major Characteristics of ARL's Thrust Augmentation Concepts	22
9.	One-Dimensional Flow Model	23
10.	Thrust Augmentation Ratio and Transfer Efficiency Versus Inlet Areas Ratio	24
	$\eta_{D11T} = 0.88$	
11.	Thrust Augmentation Ratio and Transfer Efficiency Versus Inlet Area Ratio	25
	$\eta_{D11T} = 0.92$	
12.	Thrust Augmentation Ratio and Transfer Efficiency Versus Inlet Area Ratio	26
	$\eta_{D11T} = 0.96$	
13.	Thrust Augmentation Ratio Versus Reciprocal Diffuser Area Ratio	27
14.	Thrust Augmentation Ratio Versus Transfer Efficiency for Optimum Diffuser Area Ratio	28
15.	Thrust Augmentation Ratio Versus Flight Speed Ratio I	29
16.	Thrust Augmentation Ratio Versus Flight Speed Ratio II	30
17.	Thrust Augmentation Ratio Versus Flight Speed Ratio III	31
18.	Propulsive Efficiency Versus Flight Speed Ratio I	32
19.	Propulsive Efficiency Versus Flight Speed Ratio II	33
20.	Propulsive Efficiency Versus Flight Speed Ratio III	34
21.	Thrust Augmentation Ratio Versus Transfer Efficiency for 1, 2, and 3 Stages I	35
22.	Thrust Augmentation Ratio Versus Transfer Efficiency for 1, 2, and 3 Stages II	36
23.	Thrust Augmentation Ratio Versus Transfer Efficiency for 1, 2, and 3 Stages III	37
24.	Thrust Augmentation Ratio Versus Transfer Efficiency Optimum 2-Stage I	38
25.	Thrust Augmentation Ratio Versus Transfer Efficiency Optimum 2-Stage II	39
26.	Thrust Augmentation Ratio Versus Transfer Efficiency Optimum 2-Stage III	40
27.	Thrust Augmentation Test Rig	41
28.	Thrust Augmentation Test Rig Perspective View	42
29.	Multiple Injection, Effects of Primary Nozzle Location and Off-Axis Inclination	43
30.	Experimental Measurement of Thrust Augmentation Ratio Versus Manifold Pressure Head	44
31.	Experimental Data Showing Influence of Primary Nozzle Inclination	45
32.	Thrust Augmentation For V/STOL Aircraft	46
33.	V/STOL Propulsion Chart	47
34.	V/STOL Propulsion Spectrum	48
35.	Relationships Between Thrust Augmentation Performance and Characteristic Area Ratios	49
36.	Diffuser Exit to Wing Area Ratio Versus Augmented Thrust Per Fan Horsepower I	50
37.	Diffuser Exit to Wing Area Ratio Versus Augmented Thrust Per Fan Horsepower II	51
38.	Basic Aircraft Types Employing Thrust Augmentation	52
39.	Schematic of Supersonic VTOL Aircraft with Thrust Augmentation	53
40.	Schematic View of Supersonic VTOL Aircraft	54
41.	Supersonic Aircraft — View AA	55
42.	Propulsive Wing — Suction Side	56
43.	Propulsive Wing — Pressure Side	57
44.	Artist's View of Jet Wing Aircraft	58
45.	Propulsion By Acceleration of Boundary Layer	59
46.	Shrouded Wing Configuration for Fluid Dynamic Energy Transfer to Boundary Layer	60
47.	Increase of Total Momentum By Boundary Layer Acceleration	61
48.	Non Shrouded Wing Configuration	62
49.	Hybrid Aircraft, I	63
50.	Hybrid Aircraft, II	64
51.	Fundamental Research on Thrust Augmentation	65
52.	Engineering Research on Thrust Augmentation for V/STOL	66

CONFIDENTIAL

I. INTRODUCTION

The Aerospace Research Laboratories (ARL) has a broad, fundamental research program in fluid dynamic energy transfer. This broad research field is concerned with the phenomena of direct energy and momentum exchange between fluid media of different physical characteristics. A better understanding of these phenomena plays a key role in advanced aerospace propulsion and energy conversion technology and will be especially significant for the realization of energy conversion processes that do not employ moving mechanical parts. Major research areas and associated applications of fluid dynamic energy transfer are shown in Figure 1. Studies on jet mixing and jet energy transfer at ARL led to theoretical and experimental research on the thrust augmentation process. As a result of these studies, it was found that thrust augmentation can be performed far more efficiently and at much higher augmentation levels than has ever been reported. (A comprehensive review of the state of the art in thrust augmentation is contained in Reference 5, "Steady-State Thrust Augmentors and Jet Pumps," by Peter R. Payne.)

The purpose of this report is to indicate the potential feasibility of applying ARL's thrust augmentation concepts to V/STOL aircraft propulsion systems. The enormous military and

commercial importance of V/STOL aircraft has become evident during recent years (Ref. 6); many avenues have already been explored, ranging from improvements on helicopters to novel aircraft designs with tiltable engines or wings, lift turbojets, or lift rotors located above or within the wings. The XV-4A (Lockheed Hummingbird) represents a previous effort in applying thrust augmentation to the V/STOL propulsion problem. The XV-4A program demonstrated the feasibility of thrust augmentation, but the performance of the thrust augmentor was not sufficient to achieve an aircraft competitive with other V/STOL concepts (Ref. 4).

The encouraging preliminary results at ARL (thrust augmentation ratio of 2.8) and the progress of further research efforts toward higher energy transfer efficiencies led to investigations of thrust augmentor applications for V/STOL aircraft. Various concepts evolved, some typically for subsonic, others for supersonic configurations, which indicate many potential performance advantages. Also, some favorable operational characteristics can be realized, such as low noise levels, no runway damage or surface erosion, and excellent possibilities for suppression of infra-red radiation.

CONFIDENTIAL

II. THRUST AUGMENTATION PROCESSES

The thrust augmentation process for an air-breathing propulsion system is shown schematically in Figure 2. A primary mass flow, \dot{m}_0 , is ejected with a primary velocity, v'_0 . The primary flow conditions are defined as those achieved when the primary jet is discharging into the ambient atmosphere. The primary thrust, T'_0 , and energy flow/second, L'_0 , of the ejector are defined as follows:

$$\begin{aligned} T'_0 &= \dot{m}_0 v'_0 & (1) \\ L'_0 &= \dot{m}_0 v'^0_0{}^2 & (2) \end{aligned}$$

The augmentation process occurs when the primary air is discharged into the inlet duct of the thrust augmentor schematically pictured in the right side of Figure 2. The effects of the mixing and diffusing of the primary and aspirated mass flows create a region of reduced pressure at the inlet. This pressure reduction gives the primary jet an increased velocity from v'_0 to v_0 through the nozzle of area A_0 , and also causes the aspirated mass flow, \dot{m}_1 , to enter the inlet area A_1 with a velocity v_1 . This aspirated or secondary flow then mixes with the primary jet flow in the duct behind the inlet. After mixing is completed, the total mass flow has the velocity v_2 . The mixed flow enters the diffuser section to be discharged from the diffuser to ambient pressure with a velocity v_3 . The diffuser entrance and exit areas are, respectively, A_2 and A_3 . The augmented thrust, T , and energy flow/second, L , are given below:

$$\begin{aligned} T &= (\dot{m}_0 + \dot{m}_1) v_3 & (3) \\ L &= (\dot{m}_0 + \dot{m}_1) v_3^2 & (4) \end{aligned}$$

The definitions and simple relationships given above make it possible to define the fluid dynamic energy transfer efficiency, η_{tr} .

The energy transfer efficiency is defined as the ratio of the energy flow/second, L , of the thrust augmentor system to the primary energy flow/second, L'_0 :

$$\eta_{tr} = \frac{L}{L'_0} = \left[\frac{\dot{m}_0 + \dot{m}_1}{\dot{m}_0} \right] \left[\frac{v_3}{v'_0} \right]^2 \quad (5)$$

The thrust augmentation ratio is:

$$\frac{T}{T'_0} = \left[\frac{\dot{m}_0 + \dot{m}_1}{\dot{m}_0} \right] \left[\frac{v_3}{v'_0} \right] \quad (6)$$

The quantity $(\dot{m}_0 + \dot{m}_1)/\dot{m}_0$ used in Eqs. 5 and 6 may be called the mass augmentation ratio. From Eqs. 5 and 6 the following relationships between the three thrust augmentor

performance parameters (mass augmentation ratio $(\dot{m}_0 + \dot{m}_1)/\dot{m}_0$; thrust augmentation ratio T/T'_0 ; and energy transfer efficiency (η_{tr})) can be derived:

$$\begin{aligned} \frac{T}{T'_0} &= \sqrt{\eta_{tr} \frac{\dot{m}_0 + \dot{m}_1}{\dot{m}_0}} \\ \text{or} \quad \frac{\dot{m}_0 + \dot{m}_1}{\dot{m}_0} &= \frac{(T/T'_0)^2}{\eta_{tr}} \\ \text{or} \quad \eta_{tr} &= (T/T'_0)^2 \frac{\dot{m}_0}{\dot{m}_0 + \dot{m}_1} \quad (7) \end{aligned}$$

These equations are based on the condition that the exit velocity v_3 is constant over the entire exit area A_3 . If this condition is not fulfilled, integral expressions for the energy transfer efficiency and thrust augmentation ratio may be employed. However, such expressions will not be derived here, since the thrust augmentation methods discussed in this report lend themselves to a nearly uniform exit velocity. With the thrust augmentor performance parameters and the primary gas conditions (\dot{m}_0 and v'_0), the thrust augmentor performance characteristics in terms of T'_0 ; T ; \dot{m}_0 ; \dot{m}_1 ; v'_0 ; v_3 and η_{tr} are determined. When, in addition to these performance parameters, the exit mass density, ρ_{ex} , is given, the overall exit area A_3 and the thrust density T/A_3 are determined as follows:

$$A_3 = T \frac{(T/T'_0)^2}{\rho_{ex} v'^0_0{}^2 \eta_{tr}^2} = T'_0 \frac{(T/T'_0)^3}{\rho_{ex} v'^0_0{}^2 \eta_{tr}^2} \quad (8)$$

and

$$T/A_3 = \rho_{ex} v'^0_0{}^2 \left[\frac{\eta_{tr}}{T/T'_0} \right]^2 = 2 \Delta P_{TOT} \quad (9)$$

In case the mass density is essentially constant throughout the ejector, A_3 and T/A_3 can be expressed as follows:

$$A_3 = A'_0 \frac{(T/T'_0)^3}{\eta_{tr}^2} \quad (10)$$

and

$$T/A_3 = (T'_0/A'_0) \left[\frac{\eta_{tr}}{T/T'_0} \right]^2 \quad (11)$$

When the ratio of total length of the thrust augmentor to the hydraulic diameter of the diffuser exit is also given, all of the major parameters for comparing various thrust augmentor types are known.

Significant performance improvements over the present state-of-the-art of ejector technology can be obtained from a better understanding

CONFIDENTIAL

of the principal loss mechanisms in ejectors. The total energy transfer loss in ejectors can be considered as a result of two major categories of loss mechanisms, namely:

- Drag losses due to wall surface friction and flow separation phenomena;
- Losses resulting from the mixing between primary and entrained air.

The sum of these two major loss types must be made a minimum in order to optimize the energy transfer process. The methods of achieving this and the associated typical problems vary greatly with the conditions under which the energy transfer process has to operate. These conditions can be characterized by the following parameters:

1) The physical characteristics determining the velocity of primary and entrained working media for given pressure conditions; these are the specific heat ratio, γ , the molecular weight, and the temperature. The significance of these parameters for thrust augmentation performance will be shown later in this section. Under incompressible flow conditions, the mass density becomes the only factor determining the flow velocity for given pressure conditions.

2) The ratio of primary mass flow \dot{m}_0 to the entrained mass flow \dot{m}_1 , which may range from values much smaller than one to values much larger than one.

3) The Mach number of the primary working medium entering the ejector M_{P1} , which may range from low subsonic to high supersonic values.

4) The Mach number of the entrained mass flow, M_{E1} , which may range from low subsonic to supersonic values.

5) The flow field within the ejector, which may be of essentially one-, two- or three-dimensional structure.

The specific combination of these operational conditions in each case determines whether the potential ejector performance may be poor or excellent. As one typical example, the influence of the flow field structure on the ejector performance, as mentioned under #5), above, will be discussed briefly in the following. In Figure 3, two- or three-dimensional flow fields are shown. Some of these flow field structures can be favorable; some can be very unfavorable. Von Karman (Ref. 2, 7) has shown that primary flow injection into the regime of local over-velocity near a curved ejector inlet duct can substantially reduce the mixing losses, which in turn can greatly improve the overall ejector performance. Typical examples of very

unfavorable two- or three-dimensional flow fields at the diffuser entrance are illustrated in Figure 3 B-2 and -3. Such diffuser inlet flow distortions, which result from primary gas injection methods such as illustrated in Figure 4, cause large diffuser losses. A most desirable velocity field of a flow entering a diffuser is illustrated in Figure 3 B-1, which represents an essentially one-dimensional flow field with a slight velocity increase near the diffuser walls.

Ejector configurations fully exploiting favorable two-dimensional inlet flow conditions without diffuser or with a relatively small area ratio diffuser may be capable of excellent performance. However, under the specific operational conditions which exist in the case of thrust augmentation, the essentially one-dimensional flow-type ejector seems to rank among the best conceivable types. This will be shown later in this section.

First, the major characteristics of one-dimensional type ejectors shall be discussed: One-dimensional ejector in the sense of this report means that all velocity derivatives normal to the axis disappear. This corresponds to an ejector configuration with a large multiplicity of injection nozzles and an ejector wall contour with sufficiently mild curvature to avoid distortions of the velocity profile.

Two major types of one-dimensional ejectors can be defined, namely:

- Ejectors with changing cross section during the mixing between primary and entrained gas.
- Ejectors with constant cross section during the mixing between primary and entrained gas.

The performance analysis of the ejector type with changing cross section during mixing requires knowledge of the details of the mixing process. In contrast to this, the details of the mixing process are of no importance when the flow cross section during mixing is constant. Under this condition the total momentum during the mixing process remains constant, except for the effects of shear stresses on the duct walls. This process, while not necessarily best in performance, is most suitable for an understanding of the nature of the loss mechanisms and for an analytical treatment. In Figure 5, the main loss mechanisms are illustrated for such an ejector type. The duct velocity v_1 is the only addition to the nomenclature used for the thrust augmentor of Figure 2. The duct velocity lies between the velocities v_1 and v_2 ; however, in the case of nearly incompressible flow and relatively large mass ratios, the velocities v_1 and v_2 are nearly the same. The mixing loss, or so-called impact loss, is given by

CONFIDENTIAL

the velocity differential squared times one-half the mass of the primary jet.

The inlet and mixing duct drag loss arises from skin friction in these areas. The friction loss coefficient, which is referred to the energy flow-second of the primary and entrained mass flow in the mixing duct, is a function of Reynolds number and the ratio of duct length to duct diameter. The diffuser loss corresponds to the total pressure loss of the flow through the diffuser section. This change in total pressure can be determined from the diffuser efficiency, η_{diff} and the velocities v_2 and v_3 . The equations for the above loss mechanisms are given in Figure 5. Another loss occurring under flight conditions of a thrust augmentation system would be the external fluid dynamic drag losses. However, since these losses are dependent upon the particular installation and configuration involved, they will not be treated here.

All of the losses listed above are interrelated and should be minimized according to an optimization procedure given in the next section. In this section, only some aspects of the mixing losses will be discussed. Since these losses are proportional to the velocity differential squared, this is tantamount to requiring the smallest compatible velocity differential between primary and entrained gas during mixing.

As previously stated under #1 [page 3], the physical characteristics of the primary and aspired gases play an important role in determining these mixing losses. The stagnation temperature, molecular weight and ratio of specific heats determine the speed as a function of pressure ratio. Figure 6 will aid in demonstrating the effect of these parameters upon the mixing losses. In this figure, the velocities for three different gases with different sets of values for γ , molecular weight, and temperature are plotted versus the pressure ratio. The middle curve may represent the velocity of the primary gas as a function of the ratio of driving gas pressure to static pressure at the exit of the primary nozzle. The velocities of three different types of entrained gases are represented by the three curves as a function of the ratio of ambient pressure P_{amb} to static pressure P_1 at the mixing duct entrance. The primary jet velocity v' , is shown for the pressure ratio P_0/P_{amb} . At the plane of the primary nozzle exit in the thrust augmentor, the pressure is reduced from P_{amb} to P_1 . This results in the increase of primary jet velocity from v' to the value v_0 . A vertical line is then drawn at the pressure ratio value of $(P_{amb})/P_1$. The intersection of this line with the three curves gives the

velocities of the three aspired gases entering the mixing duct. These velocities are designated v_I , v_{II} , and v_{III} . Since mixing losses are proportional to the velocity differential squared, a picture of the relative losses for these three cases may be developed. The velocity difference $(v_0 - v_I)$ is quite large so that efficiency is poor. This corresponds to the case where, for example, a rocket gas entrains ambient air into a thrust augmentor. The velocity difference $(v_0 - v_{II})$ is not so large, and efficiency will be moderately good. This corresponds to the case where both entrained and primary working media have the same physical characteristics. Finally, the velocity difference $(v_0 - v_{III})$ is quite small with a resulting very high efficiency. This corresponds to the case where a high molecular weight primary gas entrains a gas of low molecular weight, while both gases have approximately equal temperatures. Further details of these considerations can be found in Kassner's report (Ref. 3).

Figure 7 shows the various regimes of gas-gas energy transfer for different physical characteristics of the working media and for different mass augmentation ratios. For simplification, the three values γ , molecular weight, and temperature are condensed into one parameter, namely, the stagnation sonic speed $C_s = \sqrt{\frac{\gamma R_s T_s}{M}}$. Rocket thrust augmenta-

tion as previously indicated, operates in the inefficient region of small sonic speed ratios of entrained to primary gas. Thrust augmentation for air-breathing propulsion systems is in the moderately good efficiency area with sonic speed ratios near one and with medium to large mass augmentation ratios. Pumps which operate on the same principles, but with high sonic speed ratios and with small mass augmentation ratios, are in the region of high efficiency. Application to electrofluidynamics can also be accomplished with high transfer efficiency.

The specific operational conditions associated with air-breathing thrust augmentation processes can be summarized as follows:

- 1) The molecular weight; specific heat ratio, and temperature are approximately the same for both primary and entrained gas.
- 2) The ratio of entrained to primary mass flow is relatively large, on the order of magnitude 10:1.
- 3) The Mach numbers of primary and entrained gas are in the medium and low subsonic regimes, respectively. Therefore, compressibility effects are very small.

CONFIDENTIAL

Thrust augmentors for these operational conditions have been built and tested. However, the performance characteristics of these thrust augmentors, particularly the ones with rectangular cross section, did not reach values suitable for applications in the field of VTOL propulsion (Ref. 4).

It was ARL's goal to make fullest possible use of the favorable operational conditions for thrust augmentation by taking the following approach:

Achievement of a very small ratio of mixing duct length to hydraulic diameter (about one half and less). The reduction of skin friction losses by decreasing the length to diameter ratio of the mixing duct is of vital importance in achieving a high ejector efficiency. This can be seen from the analytical results given in the next section. On the other hand, decreasing the ratio of length to hydraulic diameter of the mixing duct to extremely small values (considerably below unity) makes it increasingly difficult to obtain major advantages from previously mentioned two-dimensional flow effects and also to schedule the flow cross section during mixing. Therefore, an essentially one-dimensional flow model with constant mixing duct cross section and subsequent diffuser appears to be a most realistic approach for theoretical treatment. Suitable injection means are discussed later.

Achievement of a slightly increased energization of the flow near the diffuser walls, specifically in the region of the corners. This is important for obtaining a uniform velocity distribution of the flow at diffuser exit, and a relatively short diffuser length without flow separation.

Multiple Primary Flow Injection:

Multiple primary flow injection generally entails relatively large inlet losses for both primary and entrained gas. It is the goal of ARL's multiple injection methods to achieve the following characteristics:

Configurations of primary injection means achieving a favorable velocity distribution throughout the ejector while causing a minimum inlet obstruction for the entrained air and a minimum internal flow loss of the primary air within the distribution and injection system. (Various approaches to accomplish this are discussed in a later section).

Avoidance of attenuation of the primary jets' kinetic energy at the mixing duct walls and exploitation of local deviations from essentially one-dimensional flow throughout the ejector. Resulting performance gains, as previously mentioned, are minor; they can be realized by suitable inclination and location of the primary injection means at the mixing duct inlet. Direction and distribution of primary injection means in such a manner as to accomplish a nearly uniform flow velocity profile at diffuser entrance with slightly increased velocity near the walls and corners, as previously mentioned.

Achievement of an extremely short length for the mixing of primary and entrained gas by special primary flow characteristics, nozzle shapes, and nozzle configurations.

In Figure 8, the major aspects of ARL's thrust augmentor concept are summarized, and an example of such an ejector is schematically illustrated.

CONFIDENTIAL

III. PERFORMANCE ANALYSIS OF THRUST AUGMENTATION PROCESSES

The analysis of the thrust augmentation process is tailored to ARL's concepts and will be limited to the one-dimensional flow type ejector with constant area mixing duct shown schematically in Figure 9. The combined area of the multiple injection nozzle is represented by the primary nozzle area A_0 .

Incompressibility is assumed for the entire flow, and mixing is taken to be completed at Station 2. The pressures at Stations 1, 2, and 3 are uniform over the cross sections. The nomenclature is the same as that explained in Figure 2. The analysis begins by using the integrated momentum (impulse) equation to relate the mass flows, velocities and pressures at Stations 1 and 2. Application of the continuity and energy equations reduces the momentum equation to a relation between v_1 and v_0 , with the areas A_0 , A_1 , A_2 , and A_3 , the friction loss coefficient for the inlet and mixing duct, and the diffuser efficiency as variables. The relation of v_1 to v_0 may now be used to compute the remaining velocities, the thrust augmentation ratio and the transfer efficiency. The complexity of the equations led to computer calculations, and the results are shown in Figure 10, 11, and 12. In these figures, the thrust augmentation ratio and transfer efficiency are plotted versus the ratio of inlet area to primary nozzle area A_1/A_0 . Mass augmentation ratios are not shown in these and subsequent figures since mass augmentation may be calculated from the transfer efficiency and thrust augmentation ratio (see Eq. 7). The ratio of diffuser exit area to mixing duct area, A_3/A_2 , is used as a curve parameter. For comparison only, the plot of thrust augmentation ratio for $A_3/A_2 = 1.0$ (no diffuser) is shown as a dashed line. * The diffuser efficiency, η_{diff} , is used as a sheet parameter. Diffuser efficiencies of 0.88, 0.92, and 0.96 are used in Figures 10, 11, 12, respectively. No friction losses were specified, since these losses could be accounted for by a virtual diffuser efficiency. For example, if the diffuser area ratio were $A_3/A_2 = 20$, an inlet and mixing duct friction loss coefficient of 0.03 coupled with a diffuser efficiency of 0.96 is equivalent to a virtual diffuser efficiency of 0.92. The general trend exhibited by the thrust augmentation ratio versus inlet area ratio curves is a rather large positive slope in the region of

small inlet area ratios and a much smaller slope in the region of large inlet area ratios. The plots of transfer efficiency versus inlet area ratio show efficiency rapidly dropping in the region of small inlet area ratios and then decreasing very slowly a large inlet area ratios. The curves of thrust augmentation ratio for a given diffuser efficiency, e.g., Figure 10, demonstrate that the maximum thrust augmentation for some value of the inlet area ratio (A_1/A_0) may not be the value given by the largest diffuser area ratio (A_3/A_2). This may be seen more clearly in Figure 13, where thrust augmentation ratio is plotted versus the reciprocal diffuser area ratio, A_2/A_3 , for the asymptotic case of very large inlet area ratio. The simplification of the equations in this asymptotic case permits an exact solution for the points of maximum thrust augmentation. The curve parameter shown is the diffuser efficiency and ranges from $\eta_{diff} = 1.0$ (perfect diffuser) to $\eta_{diff} = 0.88$. The dashed line gives the loci of the thrust augmentation maxima according to the equation given in the figure. These thrust augmentation maxima will be said to occur at the optimum diffuser area ratio. Figure 14 gives the thrust augmentation ratio as a function of transfer efficiency for the optimum diffuser area ratio. The curves for three sets of diffuser efficiencies and friction loss coefficients are shown to demonstrate the value of improving the system parameters. Dashed lines represent the curves of constant inlet area ratio. The experimental point at $\eta_{tr} = .25$ and $T_A/T_0 = 2.8$ was determined at inlet area ratio 182.3. This point will be discussed further in the following section. Both diffuser efficiency and friction loss coefficient are used instead of only the virtual diffuser efficiency, since these plots utilize the optimum diffuser area at each point. The value of this optimum diffuser area and the thrust produced with such a diffuser differs depending upon whether a virtual efficiency is used or whether both diffuser losses and friction losses within the mixing duct are assigned. Also, inclusion of friction losses gives more realistic results for the flight speed calculations given below. A flight system with a virtual diffuser efficiency could reduce its total loss to only the mixing loss by allowing the diffuser area to become equal to the mixing duct area.

* It should be noted, that the poor performance of the diffuserless thrust augmentor shown here is only true on the basis of the one-dimensional flow assumption. By employing favorable two-dimensional effects (Ref. 2), much higher performance values can be obtained with a diffuserless configuration than indicated in the figures.

CONFIDENTIAL

The effects of vehicle flight speed were introduced into the equations to simulate flight of a thrust augmentor and calculations were made to show these effects. Some results are shown in Figures 15, 16, 17, 18, 19, and 20. A variable diffuser was assumed so that the optimum diffuser area could be obtained at the given conditions of inlet geometry, diffuser efficiency, friction loss coefficient, and vehicle flight speed. The optimizing diffuser area ratio is largest at stillstand and decreases almost linearly with flight speed. In Figures 15, 16, and 17, the thrust augmentation ratio is plotted versus the ratio of flight speed v_f to primary velocity, v'_0 . For a fan pressure ratio of 1:48, v'_0 would be 600 miles per hour. Thus, for $v_f/v'_0 = 0.3$, v_f is 180 miles per hour. In these figures, the inlet area ratio is used as the curve parameter, and the friction loss coefficient and diffuser efficiency are used as sheet parameters. Thrust augmentors produce the best augmentation at very low speeds but can perform as well as a ducted fan system up to flight speed ratios of about 0.5 (300 miles per hour in the example given above). Large augmentation ratios at stillstand with large inlet area ratios decay rapidly with flight speed. However, moderate inlet area ratios can produce sizeable thrust augmentation with sustained performance over an appreciable speed range.

In Figures 18, 19, and 20, the overall propulsive efficiency of the thrust augmentor is plotted against the flight speed ratio for the same conditions as given in the thrust augmentation curves above. A dashed curve giving the propulsive efficiency of a non-augmented ducted fan is shown for comparison. Thrust augmentation significantly improves propulsive efficiency in the lower flight speed region. The points of intersection of the thrust augmentation curves with the non-augmented curve occur at the flight speeds where the augmented thrust is equal to that of the ducted fan. The

advantages of moderate inlet area ratios may again be seen.

Earlier efforts to achieve thrust augmentation brought forth the concept of combining two or more thrust augmentors. The combinations or stages may have varying configurations, e.g., the Melot nozzle and the Bertin ejector system (Ref. 1). An analysis of staged augmentation systems was performed at ARL to provide comparison with the single-stage system. Two different analytical methods were used. The first method was based upon the assumption that staging would act like the multiplication of equal single stages. The results of these calculations are shown in Figures 21, 22, and 23 for various diffuser efficiencies and friction loss coefficients. Two- and three-stage systems are shown along with the single-stage results. These results indicate that staging would be useful for applications with very high thrust augmentation values but relatively low transfer efficiency values.

The second method was to use the exact one-dimensional analysis of a two-stage system. Optimization of the thrust and efficiency was carried out for constant total mass flow through the two-stage system. First- and second-stage inlet and diffuser area ratios were varied to achieve the optima. The results are shown in Figures 24, 25, and 26 for various diffuser efficiencies and friction loss coefficients. The calculations show that the first, simpler method gives more pessimistic values, but that the general trend of high thrust augmentation at lower efficiency values is valid.

Various staging concepts are being investigated at ARL such as cascaded internal staging methods which promise greater compactness and greater suitability for flight applications. Analysis of staged systems in flight is in progress and experimental verification of staging is planned for the near future.

CONFIDENTIAL

IV. ARL'S TEST APPARATUS AND TEST RESULTS

The promising theoretical values presented in the previous section indicate that thrust augmentation may feasibly be applied to air-breathing propulsion systems. However, the proof of ARL's concepts and the determination of the degree to which one-dimensionality might be achieved in the laboratory had to be demonstrated experimentally. The first objectives of ARL's testing program were to provide experimental verification of:

- 1) The effectiveness of multiple injection sites with various off-axis inclinations and configurations
- 2) The theoretical predictions of the one-dimensional, incompressible flow analysis, and
- 3) The importance of flow energization at the diffuser entrance near the walls as a means of obtaining high diffuser efficiencies and preventing flow separation in relatively short diffusers.

In order to provide the greatest possible flexibility and to ensure the ability to investigate wide ranges of experimental conditions, the test apparatus was designed with all adjustable components. Both the location and direction of the multiple injection nozzles can be varied. The inlet feed ducts can also be fitted with nozzle tips of various diameters. The height of the inlet and mixing duct and also the height of the diffuser exit duct can be adjusted. The diffuser angle may be varied independently.

The possible adjustments and configurations are a quite valuable attribute of the test apparatus. However, the flexibility of the apparatus could be achieved only by accepting conditions which entail considerable performance penalties. No more than four adjustable rows of nozzles may be used without producing serious inlet obstruction. Also, the ratio of mixing duct length to hydraulic diameter is much larger than desired due to the above limitation on the number of adjustable injection sites. Some corner effects arise from the construction of the side walls.

A schematic of the test rig is shown in Figure 27, and a perspective view is given in Figure 28. The primary nozzles are mounted on four headers with 42 nozzles per header. The width of the flow channel is 60 inches throughout. The combined effects of inlet obstruction and mixing duct skin friction were estimated to give a friction loss coefficient of about 4%.

The estimated diffuser efficiency was about 94%. The entire assembly of inlet manifold, mixing duct and diffuser is mounted on a thrust stand. This thrust stand is equipped with a high-frequency shaker to keep all bearings at rolling friction levels.

Measurements are taken of the primary mass flow rate, the manifold, inlet duct and diffuser exit pressures, and the thrust. The primary thrust was measured by reversing all nozzles, erecting barriers to flow through and across the apparatus, and then determining the negative thrust generated.

An exploratory research program was initiated in early 1965 to study the effectiveness of multiple nozzle configurations and primary jet inclinations against the entrained air streamlines. The design drawings of the test ejector were completed in July, 1965, and the first test series were conducted in April, 1966. Two rows of 40 nozzles each with straight nozzle holders were used for these tests. The primary nozzles' diameter was 0.156 inch, and the mixing duct height was set at 2.5 inches. This gave an inlet area ratio of almost 100. The optimum diffuser was found to be four inches in height ($A_3/A_2 = 1.67$). The mixing duct was nine inches long so that an unfavorable large length-hydraulic diameter ratio existed. Figure 29 shows schematically the three major nozzle row configurations used. The best results were obtained with the multi-direction nozzle row (configuration C-1); the thrust augmentation ratio was about 2.2. In this configuration, the primary injection nozzles were directed to intersect the mixing duct walls about 2.5 inches upstream of the diffuser entrance. With larger or smaller off-axis inclination angles, the performance deteriorated rapidly. In configuration C-2, the thrust augmentation ratio was about 1.4.

When the primary nozzles were located at the inlet (configuration B), the best performance was obtained with a relatively strong off-axis inclination such as shown in B-1. The jet-duct wall intersection was about 5 inches upstream of the diffuser entrance. The thrust augmentation ratio for this set-up was about 2.0. When the off-axis inclination was decreased so that jets were directed toward the duct wall at the diffuser entrance, a strong buffeting of the flow was observed. Thrust augmentation of about 1.5 was observed with configuration B-2.

Injection parallel to the axis produced thrust augmentation of about 1.9 when the nozzles

CONFIDENTIAL

were 0.4 inch from the duct walls (configuration A-1). Increasing the distance from the wall caused the thrust augmentation to drop to about 1.5

The results of this exploratory research program indicated that multi-direction nozzle rows gave the best performance. Also, proper boundary layer energization through nozzle inclination was necessary for improved performance. The inclination of the primary nozzles aids in mixing, although the straight nozzle holders contribute considerable inlet obstruction. For further testing, it was decided to utilize curved nozzle holders but to continue with the single-direction nozzle rows to maintain the greatest possible experimental flexibility.

A recent series of tests used the four rows of nozzles shown in Figures 27 and 28. The mixing duct was set at six inches, and the optimum diffuser was 15 inches high (diffuser half angle of 7.2°). The primary nozzles were 0.121 inch in diameter, giving an inlet area ratio of 182. The diffuser area ratio was 2.5. The inlet manifold pressure head was varied up to 18 inches of Hg. The inlet duct pressure head ranged from 3 to 5 inches of water. A test series is presented in Figure 30. For an inlet manifold pressure of 16 inches Hg, the primary thrust was 22.7 ± 0.1 pounds. The thrust measured by the test stand was 62.0 ± 0.5 pounds, and the thrust calculated from the diffuser exit pressure integration was about 64.5 pounds. This gave a thrust augmentation ratio of 2.73 by the stand measurement and 2.84 by the exit pressure integration. Both of these points are shown in Figure 30. The low thrust augmentation values at 8 inches Hg inlet manifold pressure are due to the poorer diffuser efficiency at the lower flow velocities. This series of measurements, when compared to the one-dimensional analysis, showed excellent agreement with earlier loss and performance estimates. For example, the measurement at 16 inches Hg manifold pressure gave a thrust augmentation ratio of about 2.8. The ratio of secondary to primary mass flow was about 30, and the overall energy transfer efficiency was

about 25%. The system had a virtual diffuser efficiency of 91%. If the diffuser efficiency is taken at 94%, the friction loss coefficient was about 3%.

During the test runs, the diffuser exit pressure profile was quite uniform over a major portion of the exit duct. No dead spaces were observed, even when measurements were made in closest vicinity of the walls. A test of the effectiveness of multiple injection was made by bunching the four nozzles in the center of the inlet, simulating a central front injector. The augmented thrust for this test was only 25 pounds (thrust augmentation ratio 1.45). Another series of tests, shown in Figure 31, demonstrated the importance of flow energization by proper inclination of the injection nozzles. Although these tests were at a somewhat lower thrust level, the important trends remain unchanged at higher thrust augmentation values. The thrust augmentation ratio, diffuser outlet pressure, and inlet duct pressure all show positively the results of proper nozzle inclination.

Future investigations will include studies of ground effects and diffuser angle variations. A preliminary ground-effect experiment showed that the thrust of the system is almost independent of the height of the diffuser exit above the ground up to total blockage. Diffuser angle variation will provide experiments on relatively short, wide angle diffusers.

Based on the results obtained with the present ejector, new test apparatus designs are under study and will be constructed. Various primary injection methods will be tested. Since the primary injection will no longer be adjustable, great improvements will be obtained by drastic reduction of inlet obstruction and mixing duct length to diameter ratio. Thereby, inlet and mixing duct friction losses should be reduced to such a degree that friction loss coefficients of only 1 or 2% will be experienced. Further improved diffuser designs with flow energization near the walls should yield very short diffusers having efficiencies of 96 to 98%.

CONFIDENTIAL

V. THRUST AUGMENTATION—V/STOL COMPATIBILITY

A schematic representation of a thrust-augmented propulsion system is given in Figure 32. This propulsion system consists of a thrust augmentor (e.g., a Jet Wing) and a gas turbine driven turbo-fan. The air compressed by the fan is ducted into the thrust augmentor for take-off and transition to aerodynamically sustained flight. The thrust augmentor may be oriented horizontally as in the Jet Wing or vertically as in the XV-4A (Lockheed Hummingbird). The inlet and exit areas of the thrust augmentor may be adjustable to permit flight performance optimization, or the entire augmentor may be retracted or closed off for high speed flight. The valving shown in the figure would allow direct discharge of the fan air into the ambient atmosphere in the case of a retractable augmentor or in case structural damage occurs to the augmentor system.

The compatibility of thrust augmentation for V/STOL propulsion systems must be examined to provide insight as to the usefulness of thrust augmentation and the determination of meaningful performance criteria. Thrust augmentors may not reach the transfer efficiency obtainable with lift rotors; they provide, however, increased lift or thrust without addition of rotating machinery, requiring only a relatively small addition of weight. Other potential advantages may result from the rectangular or slot-like exit cross-section of the thrust augmentor, the possibility of overall lift increase by jet flaps and finally the possibility of vehicle boundary layer acceleration for increasing the aircraft range. However, no meaningful conclusions on the relative merits or demerits of thrust augmentors against turbomachinery can be made unless integrated systems are compared. The propulsion system characteristics, such as the ratio of fan power to aircraft takeoff weight, fan pressure ratio, thrust augmentation ratio and required energy transfer efficiency, are largely determined by the desired performance characteristics of the aircraft. Such characteristics are hovering time, flight speed, altitude and range. Figure 33 will aid in demonstrating the interplay of aircraft and propulsion performance characteristics. In this figure, thrust per horsepower is shown as a scale on the left. Corresponding values of the jet velocity and jet pressure are scaled to the right. Approximate regimes of operation for various propulsion systems are also indicated. Ducted fans are shown to operate with 0.9 to 1.7 pounds thrust/horsepower.

Increasing thrust/horsepower ratio may be thought of as a measure of increasing hovering duration. If a typical ducted fan value of 1.3 pounds/horsepower is chosen, a thrust augmentation ratio of 2.0 would provide a system with lift/horsepower of a STOL propeller. Thrust augmentation of 3.0 would provide a system with the characteristics of a VTOL propeller. The thrust augmentation required to simulate helicopter thrust/horsepower appears to be beyond the capability of presently envisioned ejector performance. Although the consideration of increased thrust/horsepower is only one factor of a V/STOL propulsion system, this consideration indicates the regime of operation of thrust augmentors. Figure 34 provides another view of the V/STOL propulsion spectrum by a three-dimensional plot of lift/horsepower, disc loading and jet diameter. Various propulsion systems are identified and the anticipated regime of thrust augmentation application is shown as a shaded area.

The performance characteristics of the aircraft are also reflected in the size of the wing and the wing loading. The significant dimensions of a thrust augmentation system are of interest for compatibility considerations and may be determined relative to the wing area. Figure 35 gives the relationships between the thrust augmentor characteristics and the wing area and wing loading. The diffuser exit area may be expressed as a function of wing area, thrust augmentation ratio, energy transfer efficiency and wing loading. Also shown in the figure is a relation between the required inlet feed duct area and the wing area. The stipulation that the inlet duct area equal to or greater than three times the primary nozzle area ensures that pressure losses in the feed system will amount to only one or two per cent. The relation between inlet duct area and wing area can only be fully evaluated for compatibility after aspect ratio and wing taper have been specified.

Figures 36 and 37 are plots of the ratio of diffuser exit area to wing area versus augmented thrust/fan horsepower. Transfer efficiency is used as the curve parameter. Wing loading values typical of COIN aircraft (40 and 60 pounds/square foot) are used as sheet parameters. Augmented thrust/fan horsepower values from 2.5 to 4.0 indicate the regime of application for thrust augmentation. A compatible diffuser to wing area ratio would be about 0.5. Thus, transfer efficiencies of 40 to 50 per cent are required.

CONFIDENTIAL

The basic aircraft types employing thrust augmentation are listed in Figure 38. As mentioned above, both vertical and horizontal ejector configurations are possible. The horizontal ejector may be used either for vectored thrust augmentation or for boundary layer acceleration. Hybrid systems employing both horizontal ejector types are also possible.

A schematic of a vertical ejector configuration is shown in Figure 39. Cold by-pass fan air is ducted to the thrust augmentor for VTOL operation. Folding diffuser walls enable the closure of the system as transition to aerodynamically sustained flight occurs. Valving means are indicated which would also allow closing of the augmentor and which would allow direct discharge of the fan air. The fan-air combustor shown would provide the aircraft with supersonic capability. The additional structural weight of such an augmentor is estimated to be about 5 per cent of the augmented liftoff thrust of the aircraft. For example, a system developing 10,000 pounds thrust in the VTOL mode of operation would add roughly 500 pounds of structural weight.

The vertical ejector configuration is developed further in Figures 40 and 41. The upper view given in Figure 40 shows the ejector located in the center of the fuselage. Two turbo-fan engines located along the outside of the fuselage produce the primary thrust. The cross section AA is shown in Figure 41. Since these two drawings are essentially schematic in nature, this configuration also holds for split or double fuselages. Ducting along the length of the fuselages supplies fan air to the staggered injection nozzles. Failure of one engine would still allow operation of the system. Diffuser flow energization would allow use of the short, wide-angle diffuser shown, giving a favorable length/hydraulic diameter ratio for the system. Fuel storage space in the fuselage is not shown, but would be possible with some rearrangement of components. The diffuser walls and secondary air inlets close for cruise operation. The principal disadvantage of this configuration is the void displacement created by the inner island necessary for the ejector. For a purely subsonic aircraft configuration, the disadvantage may be overcome by a tri-fuselage design (similar to existing COIN aircraft). The ejector system could be located between the two outer fuselages and behind the central forward fuselage. This ejector could be completely retractable once transition to horizontal flight is accomplished.

The horizontal ejector may be located at the suction or pressure side of the wing. A sche-

matic of a suction-side propulsive wing is given in Figure 42. Locating the thrust augmentor at the suction side has the potential advantage of additional thrust augmentation by Coanda effect. The wing section in Figure 41 has the primary injection at the front entraining mass flow over the chord length. The diffuser area control is independent of thrust vectoring. When the thrust vectoring flap is lowered, the flow is deflected downward. A low-pressure, high velocity region develops at the point of greatest curvature. Injection of primary mass at this site will prevent separation of flow over the flap and can be accomplished with great efficiency. Additional mass is entrained into the low-pressure curved flow region, further augmenting the thrust. This suction-side propulsive wing may be used either with a single-fuselage aircraft or the tri-fuselage COIN type mentioned above.

A wing section of a pressure-side augmentor is shown in Figure 43. Diffuser area control is directly coupled with the thrust vectoring flaps. Injection of primary mass along the diffuser walls prevent flow separation. An artist's sketch of an aircraft employing such a Jet Wing is shown in Figure 44. This aircraft should hover as well as a VTOL-propeller powered type with only slightly higher specific fuel consumption and should perform in flight nearly as well as a ducted fan aircraft with a slight performance penalty due to the added structural weight and drag of the Jet Wing. The previously mentioned cascaded, internal staging method may be applicable to the Jet Wing. The primary air pressure would be higher than in the case of a single-stage ejector so that ducting problems would be greatly alleviated. Also, thrust augmentation performance and maximum flight speed would be increased.

An interesting and different method of thrust augmentation is that of energy transfer to the vehicle boundary. This method promises to maintain thrust augmentation up to high flight speeds. However, at zero flight speed, thrust augmentation will be considerably below that attainable with the previously described thrust augmentation methods. A propulsive efficiency for boundary layer acceleration is defined in Figure 45. For boundary layer profiles following a power law, it is immediately obvious that the propulsive efficiency is greater than one. However, boundary layer acceleration cannot be applied to the whole lifting body so that such efficiency levels will not be realized. Even so, boundary layer acceleration will be a highly efficient process.

CONFIDENTIAL

A wing configuration with thrust augmentor at the end portion of the wing is illustrated in Figure 46. Since the maximum profile thickness is near the end of the wing, a profile suitable for extending laminar flow over a large portion of the chord length can be employed. Due to the aspiration of wing boundary layer (see Figure 47), the velocity of the entrained air near the shroud will be considerably higher than that in the center portion. This two-dimensional flow condition can be exploited very effectively to obtain a high energy transfer efficiency by mixing the primary jets first with the high energy air near the shroud and, subsequently with the lower energy air in the center region of the thrust augmentor. This can be accomplished by an inward inclination of the elliptical or slot-like injection nozzles, as illustrated in Figure 47. In order to allow a crossing of the primary jets in the central portion of the thrust augmentor, the two rows of elliptical primary injection nozzles are staggered. In Figure 48, a nonshrouded thrust augmentation configuration with aerodynamic characteristics similar to those of the shrouded configuration is illustrated.

The main purpose of vehicle boundary layer acceleration by a thrust augmentation process is to increase the overall propulsive efficiency

and thereby the range of the aircraft, and also to increase the take-off thrust and aerodynamic lift which may result in a STOL capability. It is evident that the potential aircraft range increase will be largest if boundary layer acceleration is employed not only at the wing but also at other components of the airframe, for example, the fuselage. The above-described method of exploiting multi-dimensional flow effects for efficient acceleration of the vehicle boundary layer may also be of great interest for water propulsion. Attractive applications are for torpedoes and submarines, where a very low noise level is of great importance.

A very attractive application of thrust augmentation for subsonic and transonic aircraft appears to be a hybrid between the two previously-discussed energy transfer methods (see Figure 38; II, C). In a hybrid system, thrust augmentation is accomplished by energy transfer to the undisturbed air for vertical or short take-off and landing; during aerodynamic flight, energy transfer to the vehicle boundary layer is employed. Hybrid V/STOL aircraft with very favorable values of lift to power, lift to drag, structural weight, and overall propulsive efficiency under cruise conditions can be achieved. The hybrid system is illustrated in Figures 49 and 50.

CONFIDENTIAL

VI. LONG-RANGE FUNDAMENTAL AND ENGINEERING RESEARCH

The ejector configurations investigated in this report represent only one approach to the broad field of potential thrust augmentation processes. Other methods of fluid-dynamic energy transfer are conceivable but not well understood at the present time. In order to advance ARL's present thrust augmentation concepts and to provide a basis for evaluation and systematic investigation of future methods, a long-range fundamental research program in thrust augmentation was established in ARL. This program is outlined in Figure 51.

One important research area of immediate interest is the phenomena of primary jets mixing with aspired gases. A major research objective is the determination of methods for reducing the length required for mixing. Specifically, mixing phenomena will be investigated under conditions such as the following:

1. Effects of inclination of individual primary jets against the aspired air streamlines; the influence of the shape of the primary nozzles - circular, rectangular, or slot; orientation of the slot axis relative to the ejector walls; distorted rectangular shapes to introduce swirl by jet-flap effects; serrated trailing edges of the primary nozzles - straight or bent.

2. Effects of slight swirl in the primary jets issuing from circular nozzles; the influence of alternating swirls in multiple nozzle arrangements forming a stable swirl matrix.

3. Effects of the location and direction of primary jet nozzles located at the ejector side walls or distributed throughout the ejector inlet.

4. Effects of unsteady or cyclic primary injection methods.

Boundary layer phenomena associated with thrust augmentation in both internal and external flows are not well understood. Much work is needed to determine the role of boundary layer effects in ejector applications, for example, effects on diffuser efficiencies and optimum diffuser angles.

Work is in progress and will continue on thrust augmentation flow models. Compressibility effects and property variations between primary and aspired flows are being studied at the present. Deviations from flow one-dimensionality in actual ejectors will occur due to requirements for compactness. If such deviations

were ignored, unnecessary penalties would occur in thrust augmentor operation. Internal or shrouded ejectors will be studied fully; however, the combination of such ejectors with slots and flaps to utilize Coanda effect must be included in the program.* The operation of purely external or unshrouded augmentor configurations has previously been quite disappointing. Fundamental research on the problems of externally induced flows is sorely needed before a final judgment may be made. The relative merits of single-stage versus multi-stages have been partially explored, and further research remains to complete the comparison. As mentioned previously, energy transfer to undisturbed flow and to the vehicle boundary layer must both be investigated.

A long-range engineering research program, complementary to the fundamental research, is shown in Figure 52. Thrust vectoring methods with double and single flaps must be studied in terms of both performance characteristics and overall V/STOL compatibility. Inlet configurations compatible with both still-stand and flight conditions must be developed. Wind tunnel investigations will be required to demonstrate the flight performance of ejector configurations. The engine and propulsion system-airframe integration problems will require a great deal of ingenuity and creative engineering. Research on demonstrator aircraft and on novel aircraft system concepts is required to achieve the full potential of thrust augmentation.

The programs shown in Figures 51 to 52 represent ARL's present vision of thrust augmentation research. However, in research, many unexpected events occur, and new avenues for fluid dynamic energy transfer may appear which have not yet been imagined.

The ultimate goal of the integrated Thrust Augmentation-V/STOL Aircraft Research Program is to achieve an aircraft system with the following combined characteristics:

Negligible structural weight penalty for producing the V/STOL lift.

Hovering nearly as economically as a gas turbine powered helicopter.

Cruising as efficiently as a conventional aircraft.

Extremely low noise level.

* Personal communication from Dr. B. H. Goethert, The University of Tennessee Space Institute, February 1967.

REFERENCES

1. Guienne, P., "Les Trompes, ou L'aile-Trompe, Appliquees au Decollage Court," Jahrbuch, 1960 der WGL (Report presented to the 4th European Aeronautics Congress, Cologne, 18-22 September 1960)
2. von Karman, Theodore, "Theoretical Remarks on Thrust Augmentation," Reissner Anniversary Volume, 1949, p 461
3. Kassner, Rudolph R., and Gobetz, Frank W., "Performance of the Ducted Rocket," ASME Paper 60-AV-25, Presented at the Aviation Conference in Dallas, Texas, June 5-9, 1960
4. Nicholson R., and Lowry, R., "XV-4A VTOL Research Aircraft Program," USAAV Labs., Technical Report 66-45, May 1966
5. Payne, Peter R., "Steady-State Thrust Augmentors and Jet Pumps," USAAV Labs. Technical Report 66-18, March 1966
6. United States Air Force, Air Force Systems Command Report "Beyond the Horizon, Flight in the Atmosphere, 1975-1985," Vol. III: Vertical Take-Off and Landing, January 1967, Bernard Lindenbaum, Chairman
7. Ibid, Vol III Annexes: Vertical Take-Off and Landing, Annex K: "Ejector Technology" by Morton Alperin, January 1967

FLUID DYNAMIC ENERGY TRANSFER

A. TYPES OF PROCESSES:

(1) ENERGY TRANSFER BY WAVES

(2) ENERGY TRANSFER BY SHEAR AND/OR MIXING BETWEEN

• GAS ↔ GAS

• GAS ↔ LIQUID

• GAS ↔ TWO-PHASE FLUID

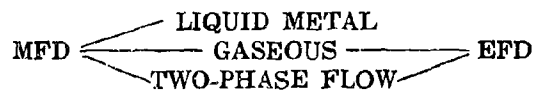
• LIQUID ↔ LIQUID

{ PARTICLES OR DROPLETS IN GAS
BUBBLES IN LIQUID

B. POTENTIAL APPLICATIONS:

(1) SHOCK TUBES; COMPREX; WAVE SUPERHEATER

(2) ADVANCED DIRECT ENERGY CONVERSION (NUCLEAR-ELECTRIC)



THRUST AUGMENTATION FOR V/STOL; ROCKETS

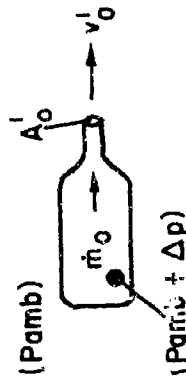
TRUE TEMPERATURE HYPERSONIC FLOW SIMULATION

(LOW MOLECULAR WEIGHT DRIVER GAS $\begin{cases} \text{AIR} \\ \text{LIQUID AIR DROPLETS} \end{cases}$)

Figure 1

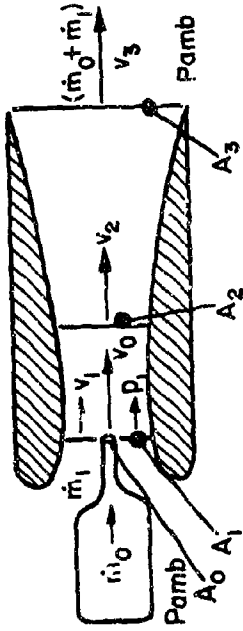
DEFINITIONS AND RELATIONS IN THRUST AUGMENTATION PROCESSES

PRIMARY MASS FLOW \dot{m}_0
DISCHARGING INTO AMBIENT
ATMOSPHERE:



PRIMARY THRUST $T'_0 = \dot{m}_0 v'_0$
PRIMARY ENERGY /sec $L'_0 = \dot{m}_0 v'^2_0$

PRIMARY MASSFLOW DISCHARGING INTO
THRUST AUGMENTOR:



\dot{m}_1 = ASPIRED MASSFLOW
AUGMENTED THRUST $T = (\dot{m}_0 + \dot{m}_1) v_3$
ENERGY /sec $L = (\dot{m}_0 + \dot{m}_1) \frac{v_3^2}{2}$

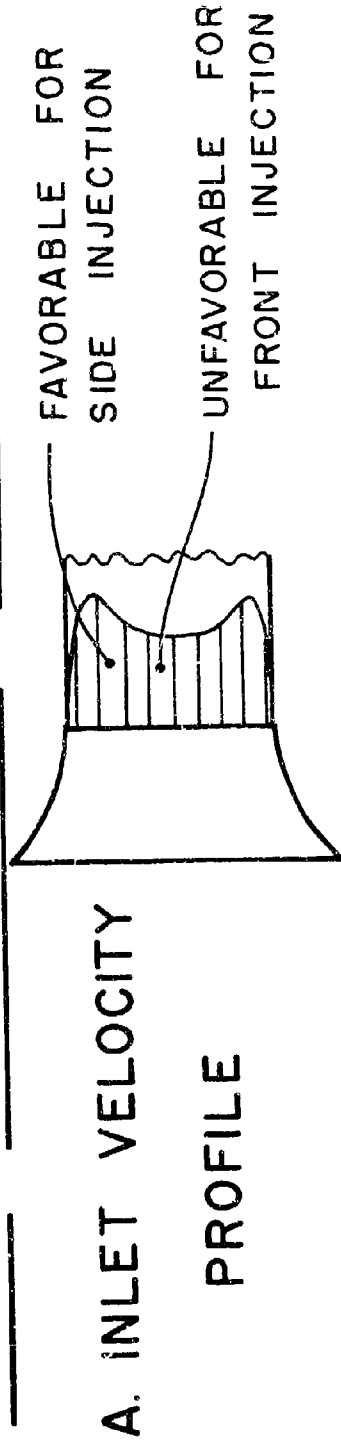
FLUID DYNAMIC ENERGY TRANSFER EFFICIENCY $\eta_{tr} = L/L_0 = \frac{\dot{m}_0 + \dot{m}_1}{\dot{m}_0} \cdot \frac{v_3^2}{v_0'^2}$

THRUST AUGMENTATION RATIO $\frac{T}{T'_0} = \frac{\dot{m}_0 + \dot{m}_1}{\dot{m}_0} \cdot \frac{v_3}{v_0'} = \sqrt{\frac{\dot{m}_1 + \dot{m}_0}{\dot{m}_0} \eta_{tr}}$

MOST IMPORTANT GEOMETRIC PARAMETERS: $\frac{A_1}{A_0} ; \frac{A_2}{A_3}$

Figure 2

MULTI DIMENSIONAL FLOW EFFECTS



B. DIFFUSER ENTRANCE VELOCITY PROFILES

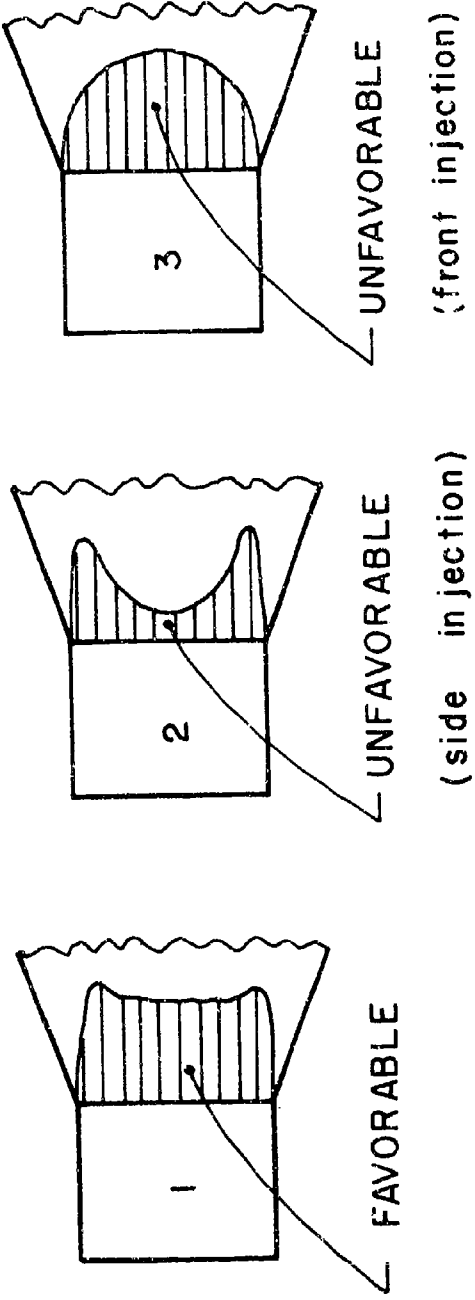


Figure 3

STRAIGHT FLOW EJECTORS
(CYLINDRICAL, ANNULAR, RECTANGULAR)

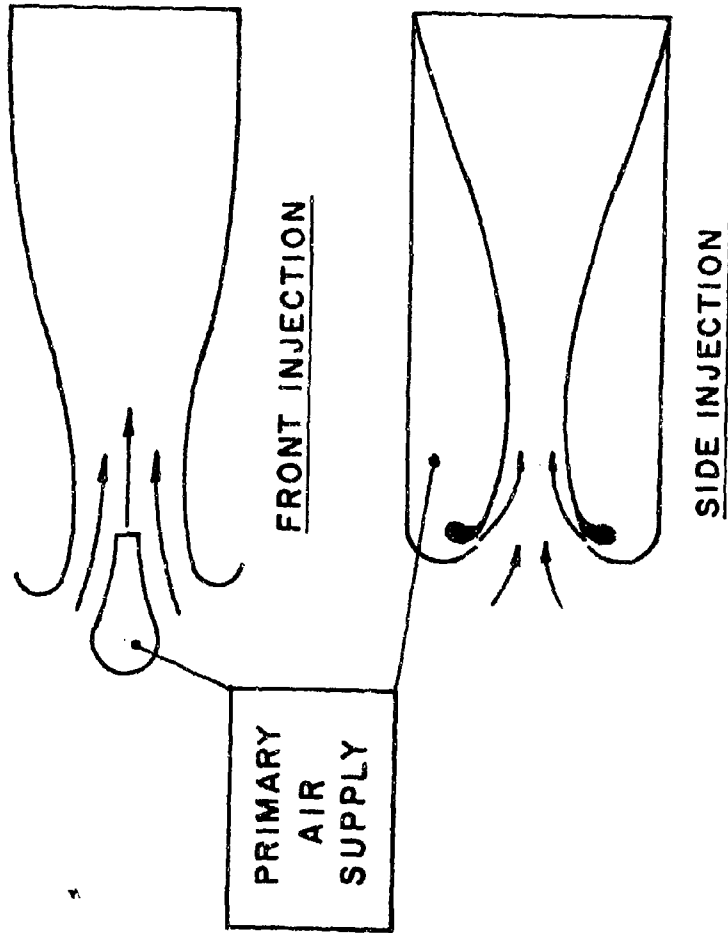
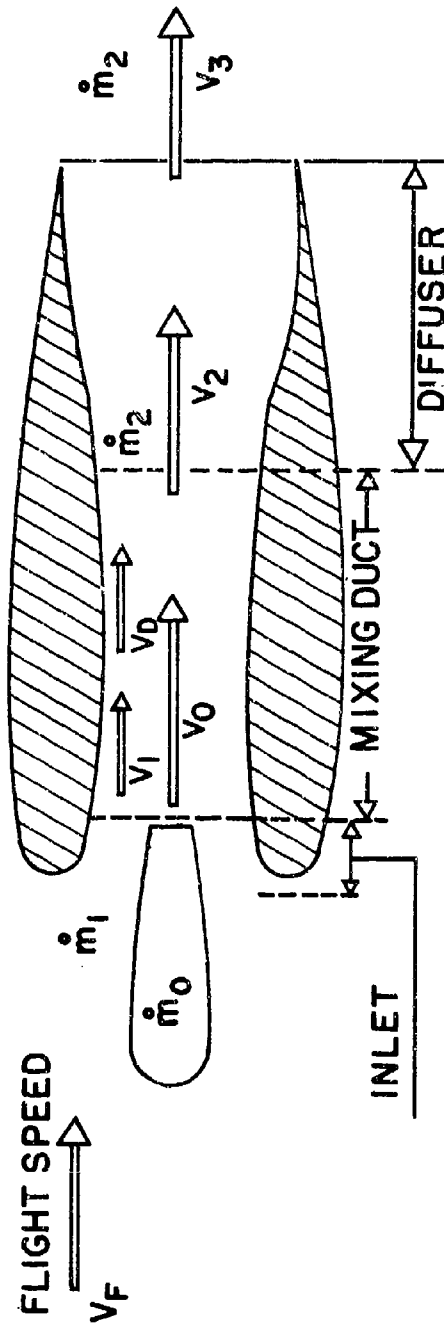


Figure 4

MAIN LOSSES IN THRUST AUGMENTATION PROCESSES



CONFIDENTIAL

- MIXING (IMPACT) LOSS: $L_m = \dot{m}_0 \frac{(V_0 - V_D)^2}{2}$
- INLET AND MIXING DUCT DRAG LOSS $L_{Dr} = \xi_{Dr} \cdot \dot{m}_2 \cdot \frac{V_D^2}{2} ; \left\langle \xi_{Dr} = F \left(Re; \frac{\text{DUCT LENGTH}}{\text{DUCT DIA.}} \right) \right\rangle$
- DIFFUSER LOSS: $L_{Diff} = (1 - \eta_{Diff}) \cdot (\dot{m}_0 + \dot{m}_1) \cdot \frac{V_2^2 - V_3^2}{2}$
- EXTERNAL FLUID DYNAMIC DRAG LOSSES

Figure 5

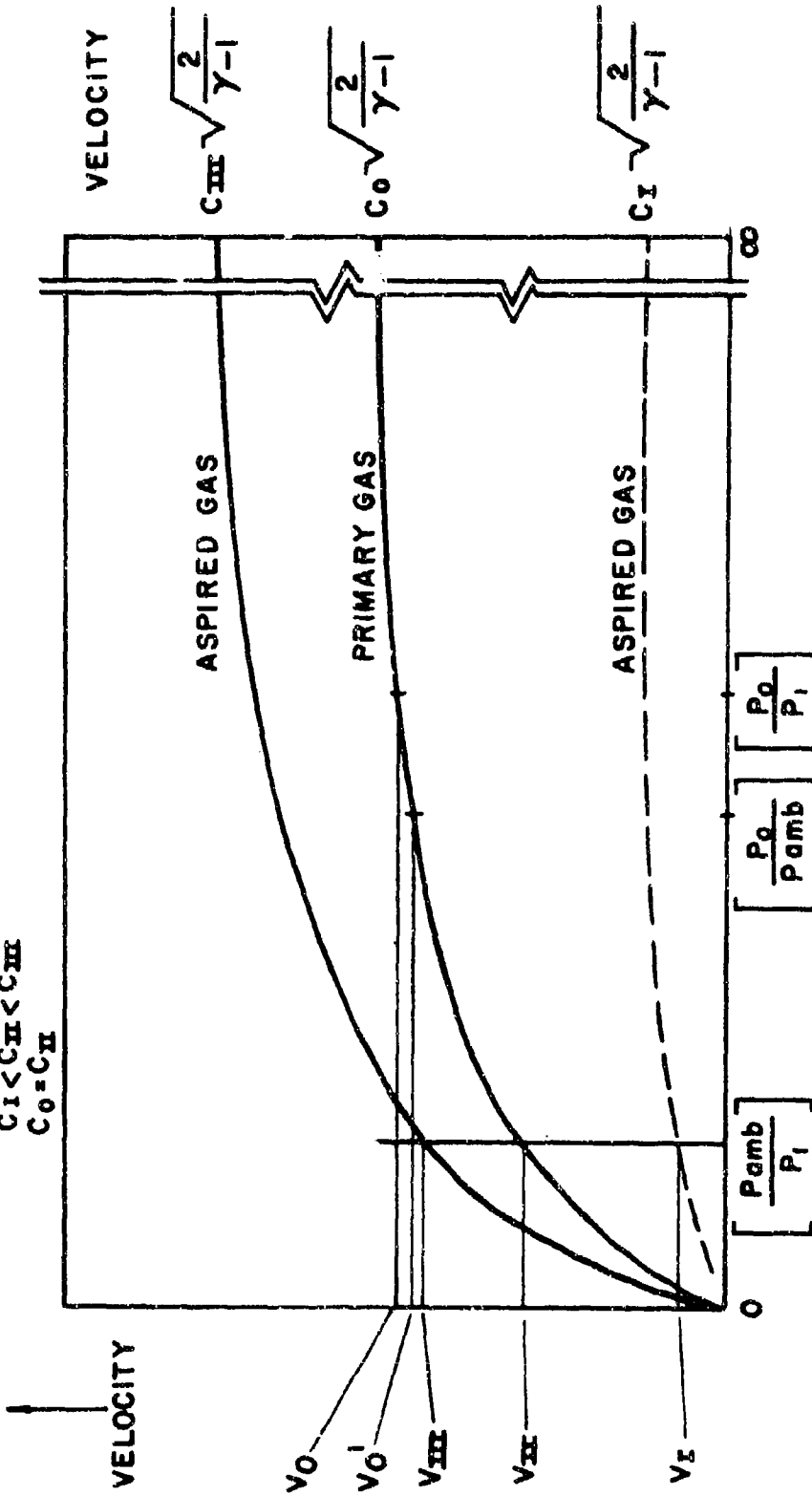
CONFIDENTIAL

VELOCITY VERSUS PRESSURE RATIO FOR GASES OF DIFFERENT SONIC SPEEDS

$$V_{MAX} = C \sqrt{\frac{2}{\gamma-1}} \quad C = \text{SONIC SPEED} = \sqrt{\frac{\gamma T}{M}}$$

$$C_I < C_{II} < C_{III}$$

$$C_0 = C_{II}$$



PRESSURE RATIO →

Figure 6

CONFIDENTIAL

CONFIDENTIAL

Figure 7 Gas - Gas Energy Transfer

Ratio of Aspired Mass Flow / Primary Mass Flow		Sonic Speed Ratio of Primary Gas/Aspired Gas $\sqrt{\gamma T/m_{prin}(0)} / \sqrt{\gamma T/m_{aspired}(1)}$		
		$>> 1$	≈ 1	$<< 1$
SMALL $m_1/m_0 = 1$	ROCKET			HIGH PRESSURE RATIO EJECTOR PUMPS
MEDIUM $m_1/m_0 = 1 \rightarrow 10$	THRUST		AIR BREATHING THRUST AUGMENTATION PROCESSES FOR V/STOL	RECIRCULATORY ELECTRO FLUID DYNAMIC PROCESSES
LARGE $m_1/m_0 > 10$	AUGMENTATION			

MAJOR CHARACTERISTIC OF ARL'S THRUST AUGMENTATION CONCEPTS

- MAJOR CHARACTERISTIC OF ARL'S THRUST AUGMENTATION CONCEPTS (RAPID MIXING)
- MULTIPLICITY OF PRIMARY INJECTION MEANS (CIRCULAR OR SLOT-TYPE INJECTION; RAPID MIXING)
- NO ATTENUATION OF PRIMARY JETS AT MIXING DUCT WALLS
- SLIGHT INCLINATION OF PRIMARY JETS TOWARD DIFFUSER WALLS FOR SLIGHT FLOW ENERGIZATION
- SLIGHT INCLINATION OF PRIMARY JETS TOWARD DIFFUSER WALLS FOR SLIGHT FLOW ENERGIZATION
- SUFFICIENT FOR COMPLETION OF MIXING
- MIXING DUCT LENGTH LARGER THAN DUCT LENGTH ($D_{hydraulic} < L$)
- HYDRAULIC DIAMETER OF MIXING DUCT LARGER THAN DUCT LENGTH
- SMALLEST POSSIBLE INLET OBSTRUCTION DUE TO PRIMARY INJECTION MEANS
- AUGMENTOR INLET CONFIGURATION COMPATIBLE WITH STILL STAND AS WELL AS WITH HIGH SPEED FLIGHT

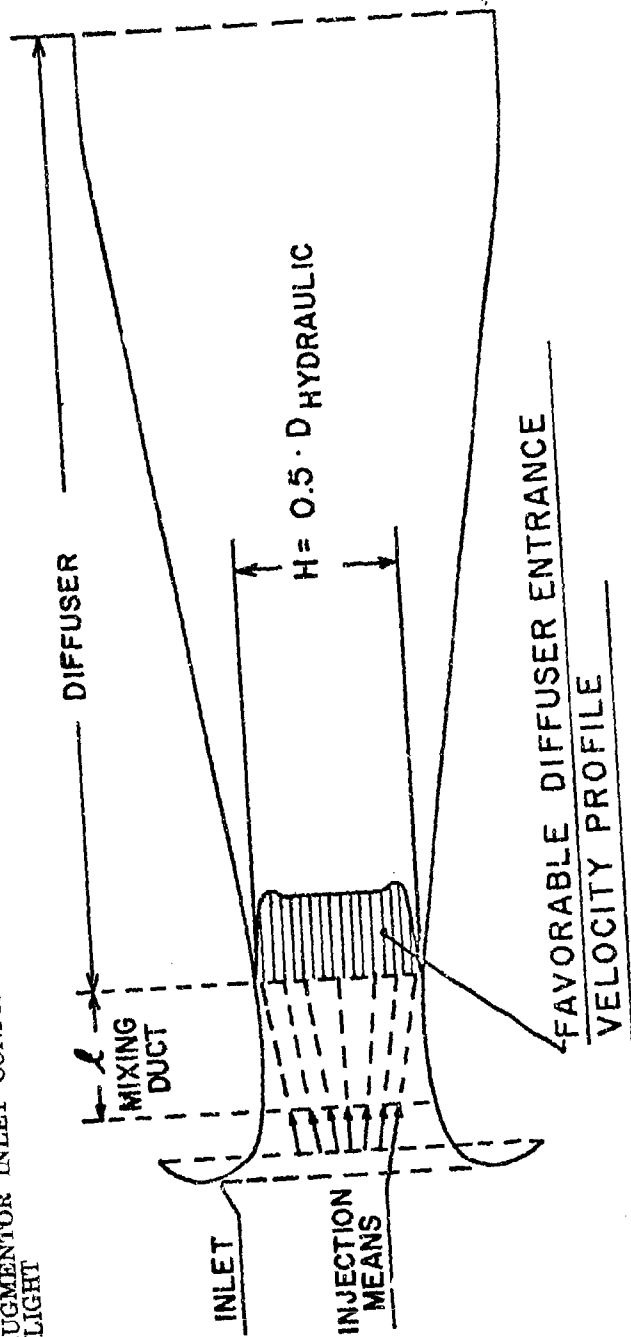


Figure 8

ONE-DIMENSIONAL FLOW MODEL

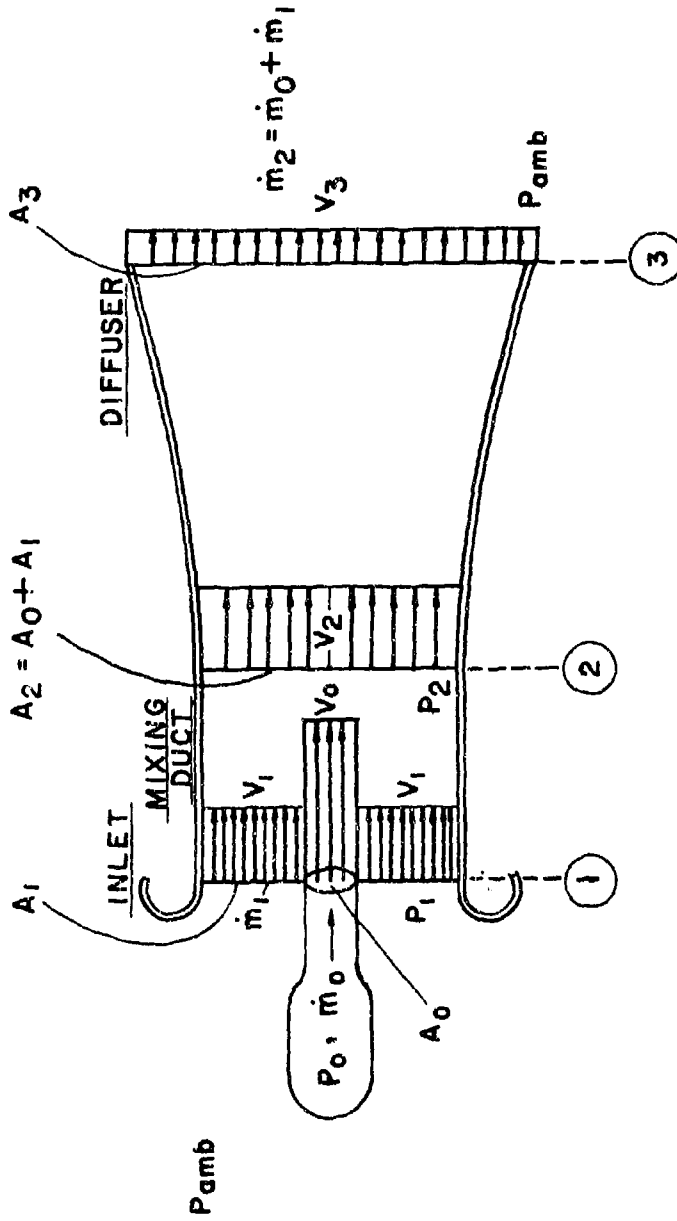


Figure 9

THRUST AUGMENTATION RATIO, T_A/T_0 , AND TRANSFER EFFICIENCY, η_{tr} , VERSUS INLET AREA RATIO, A_1/A_0 . CURVE PARAMETER: DIFFUSER AREA RATIO, A_3/A_2

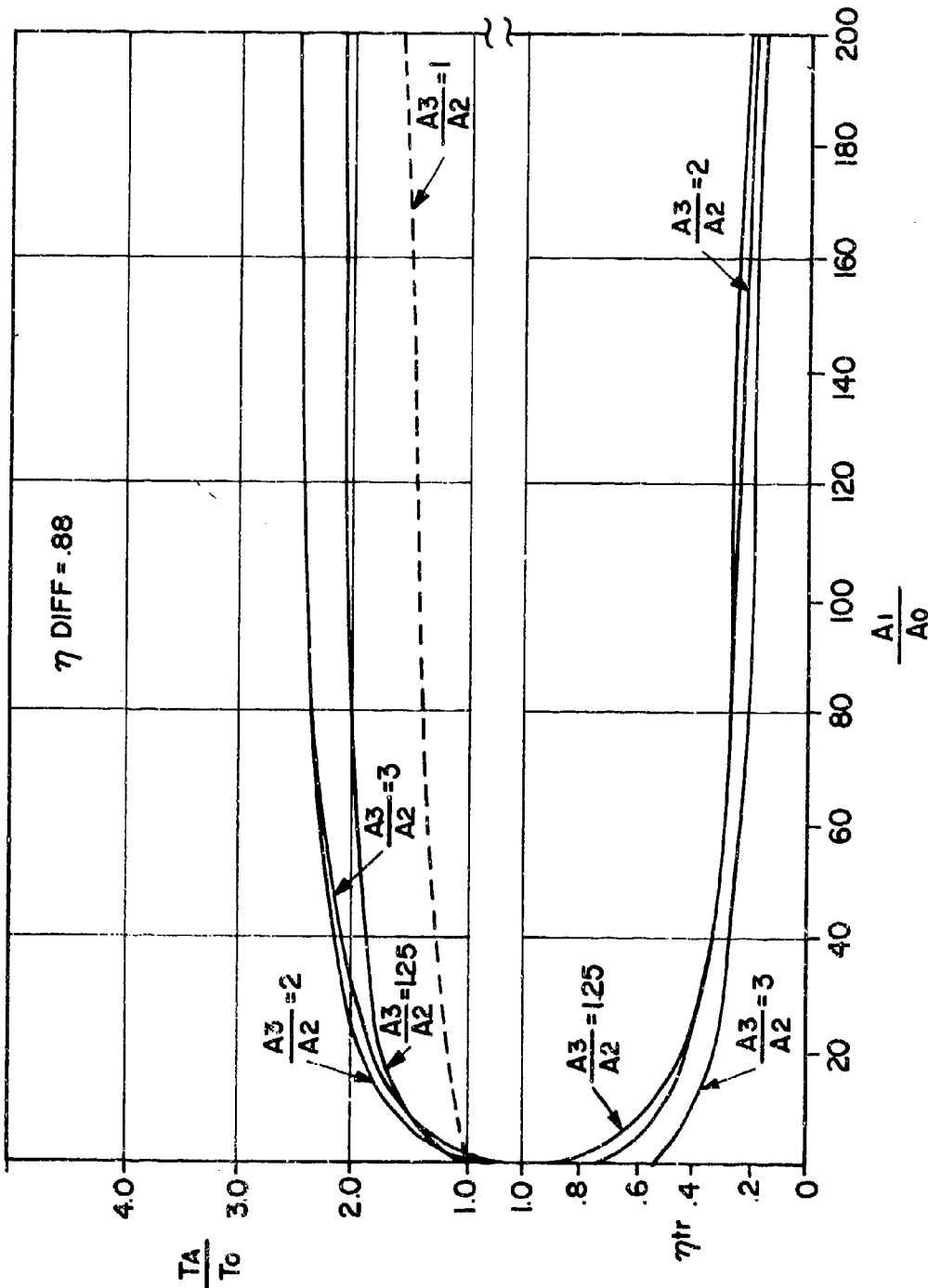


Figure 10

THRUST AUGMENTATION RATIO, T_A/T_0 , AND TRANSFER EFFICIENCY, η_{tr} , VERSUS INLET AREA RATIO, A_1/A_0 . CURVE PARAMETER: DIFFUSER AREA RATIO, A_3/A_2

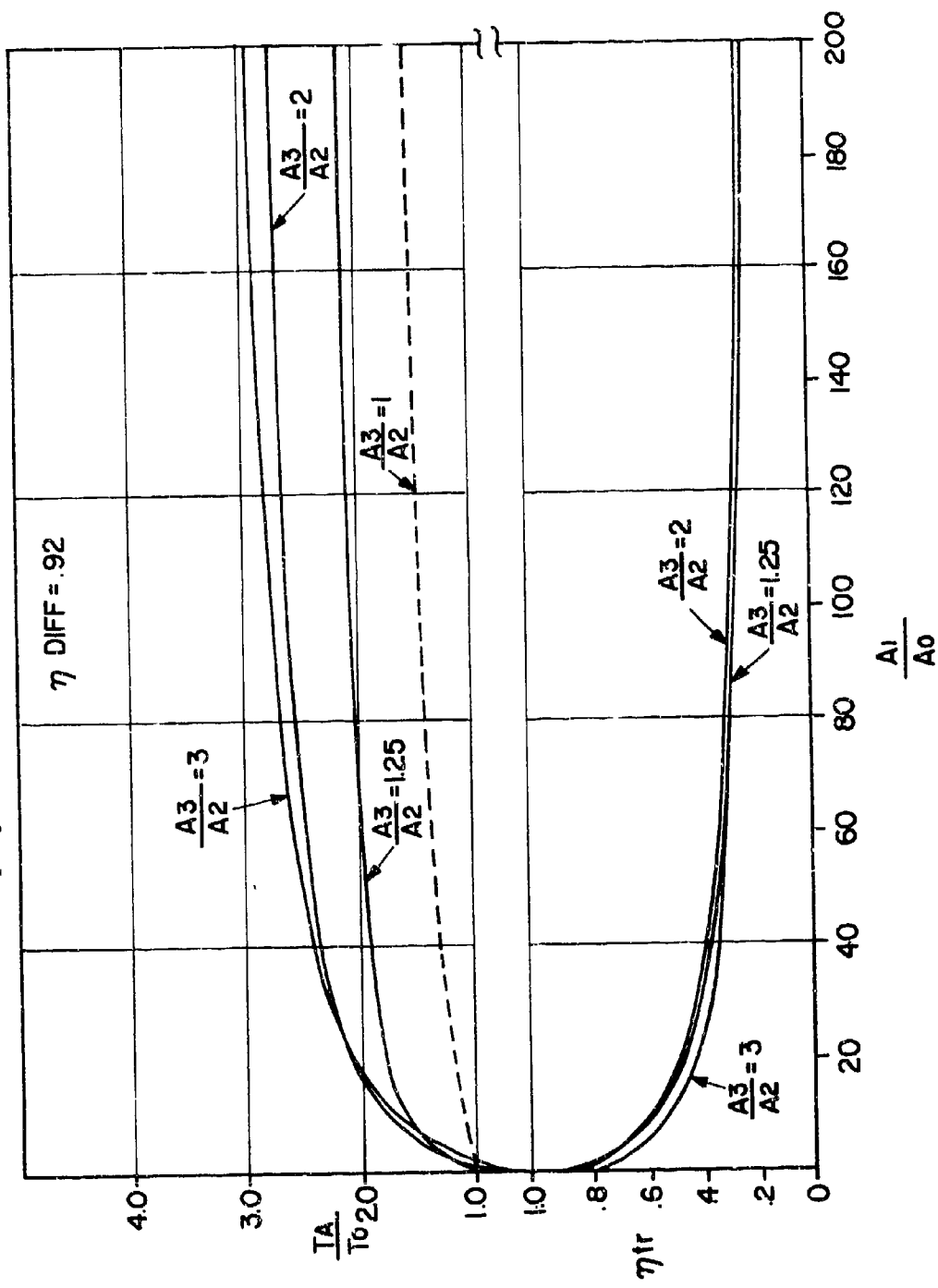


Figure 11

THRUST AUGMENTATION RATIO, T_A/T_0 , AND TRANSFER EFFICIENCY, η_{tr} , VERSUS INLET AREA RATIO, A_1/A_0 . CURVE PARAMETER: DIFFUSER AREA RATIO, A_3/A_2

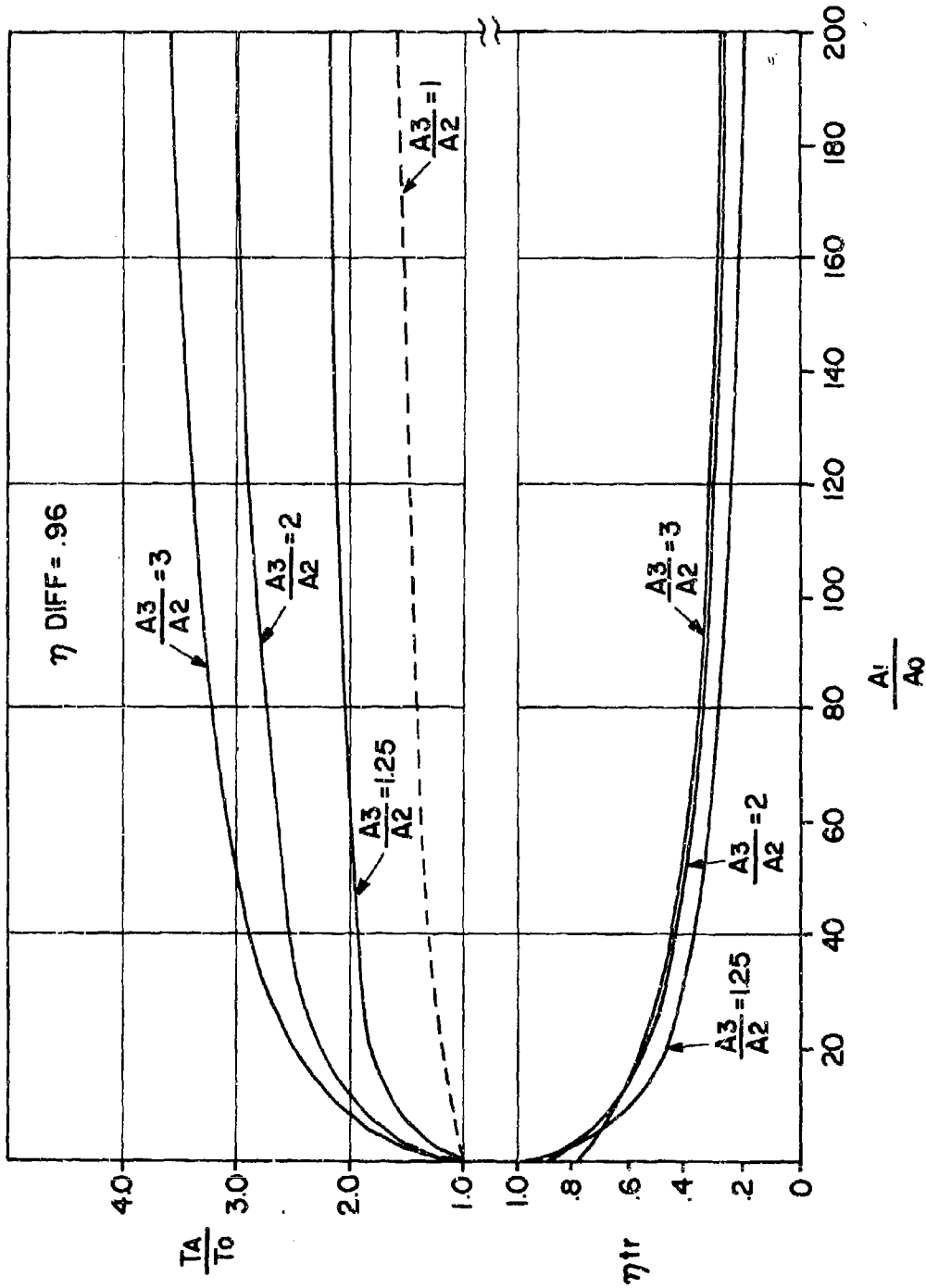
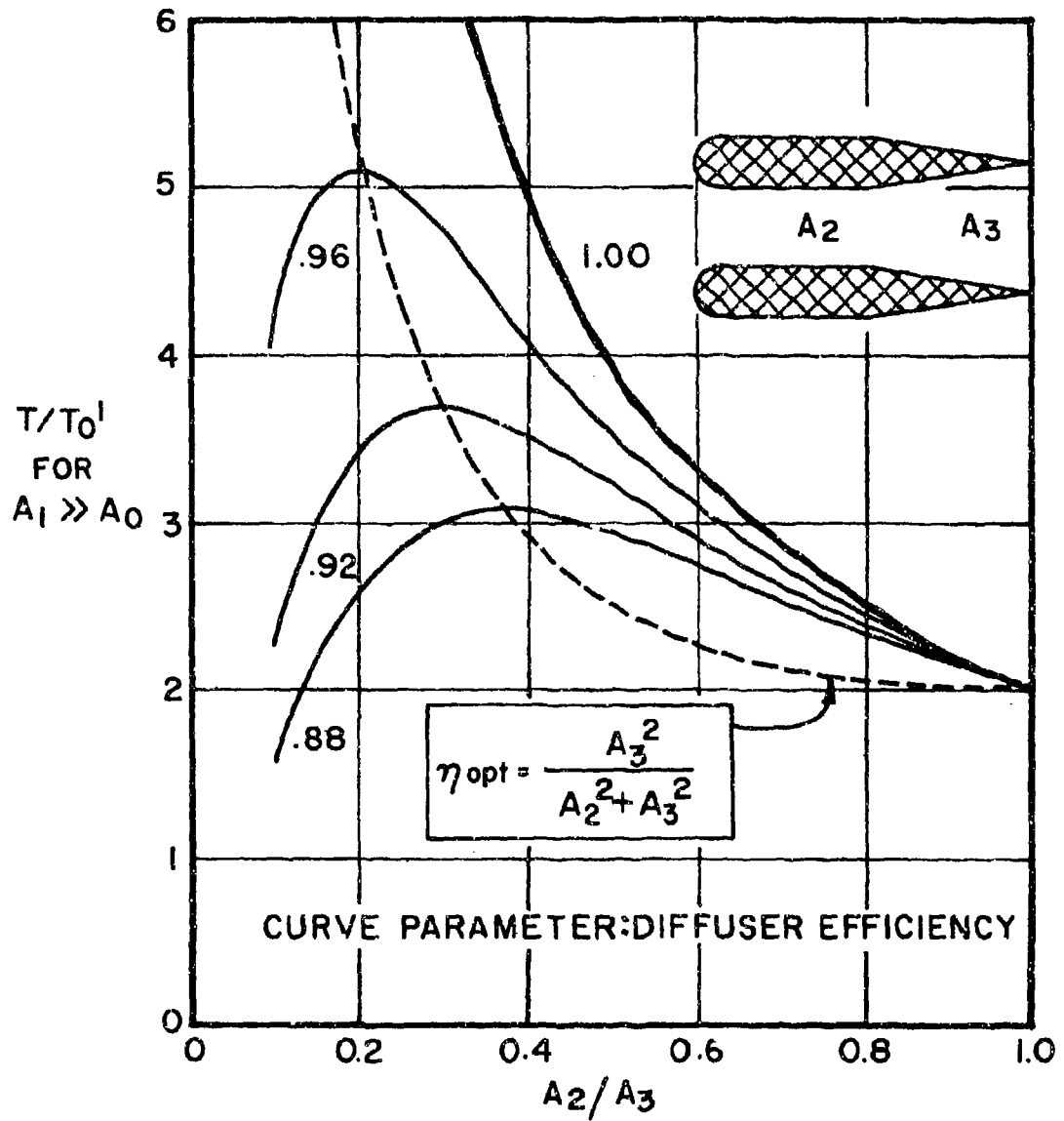


Figure 12

CONFIDENTIAL

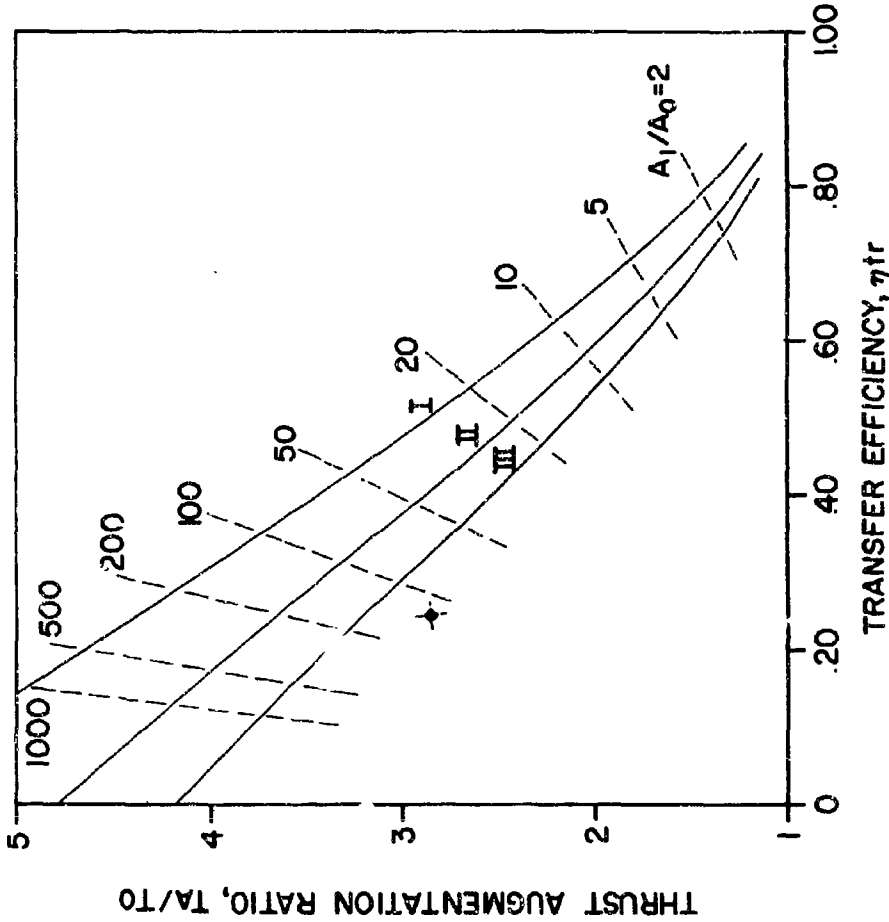
THRUST AUGMENTATION RATIO VERSUS RECIPROCAL DIFFUSER AREA RATIO.

Figure 13



CONFIDENTIAL

	CURVE I	CURVE II	CURVE III
DIFFUSER EFFICIENCY	0.98	0.97	0.96
FRICTION LOSS COEFFICIENT	0.010	0.015	0.020

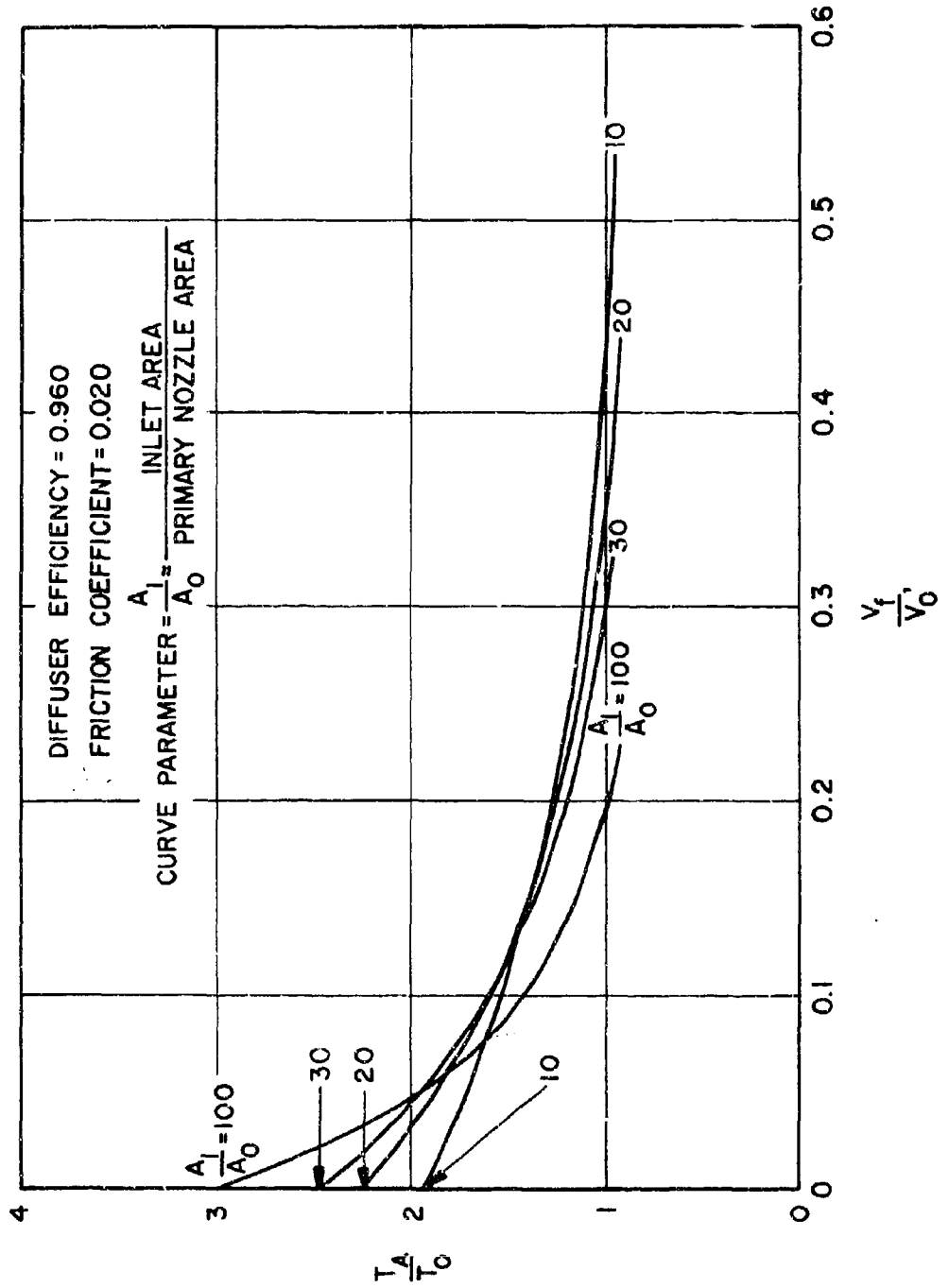


THRUST AUGMENTATION RATIO VS TRANSFER EFFICIENCY, THREE CASES. DASHED CROSS CUTS FOR EQUAL INLET AREA RATIOS, A_1/A_0 . OPTIMUM DIFFUSER AREA RATIO TAKEN ON ALL CURVES.

Figure 14

THRUST AUGMENTATION RATIO VERSUS FLIGHT SPEED RATIO. I.

Figure 15



CONFIDENTIAL

THRUST AUGMENTATION RATIO VERSUS FLIGHT SPEED RATIO. II.

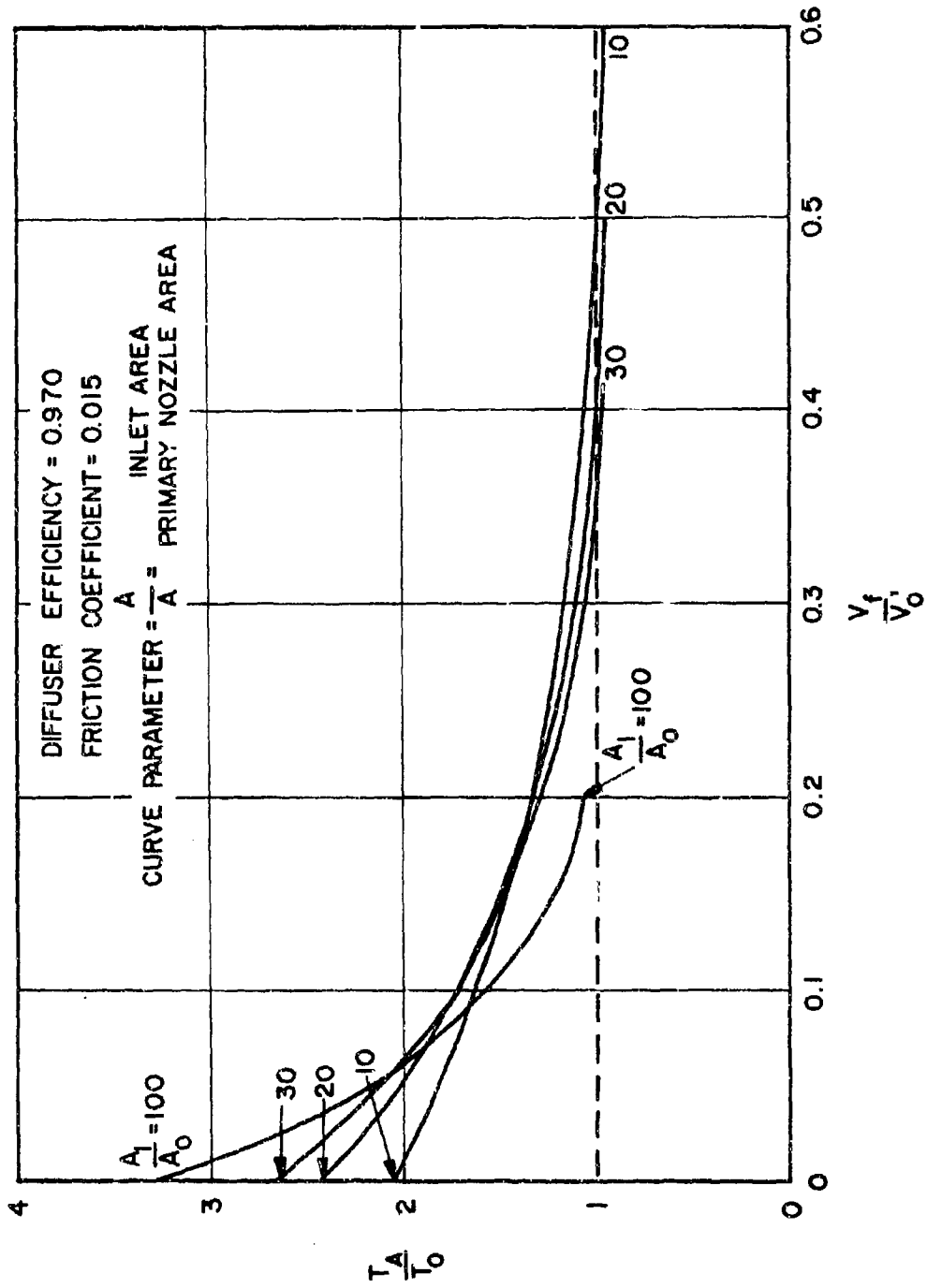


Figure 16

CONFIDENTIAL

THRUST AUGMENTATION RATIO VERSUS FLIGHT SPEED RATIO. III.

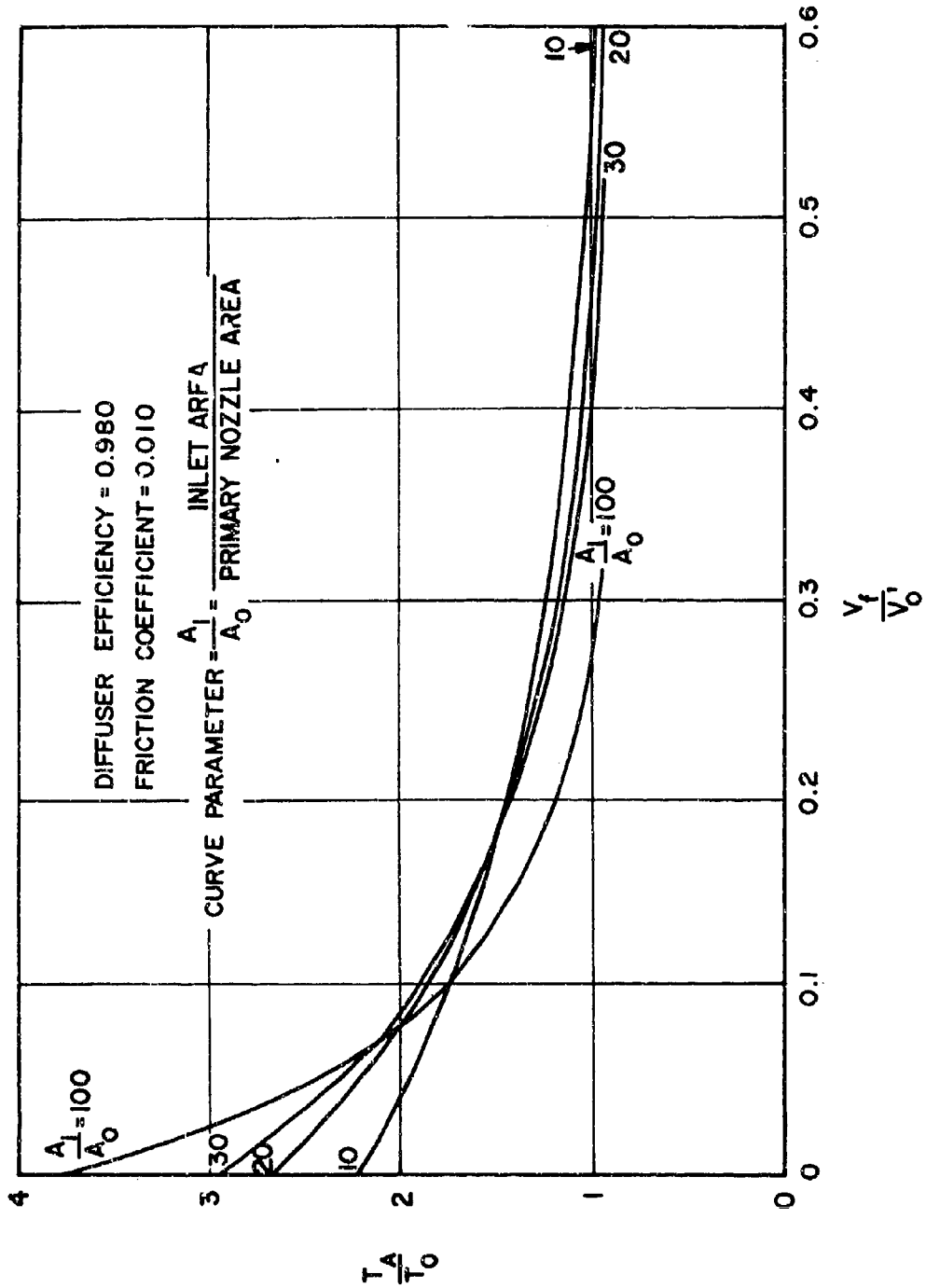


Figure 17

PROPULSIVE EFFICIENCY VERSUS FLIGHT SPEED RATIO. I.

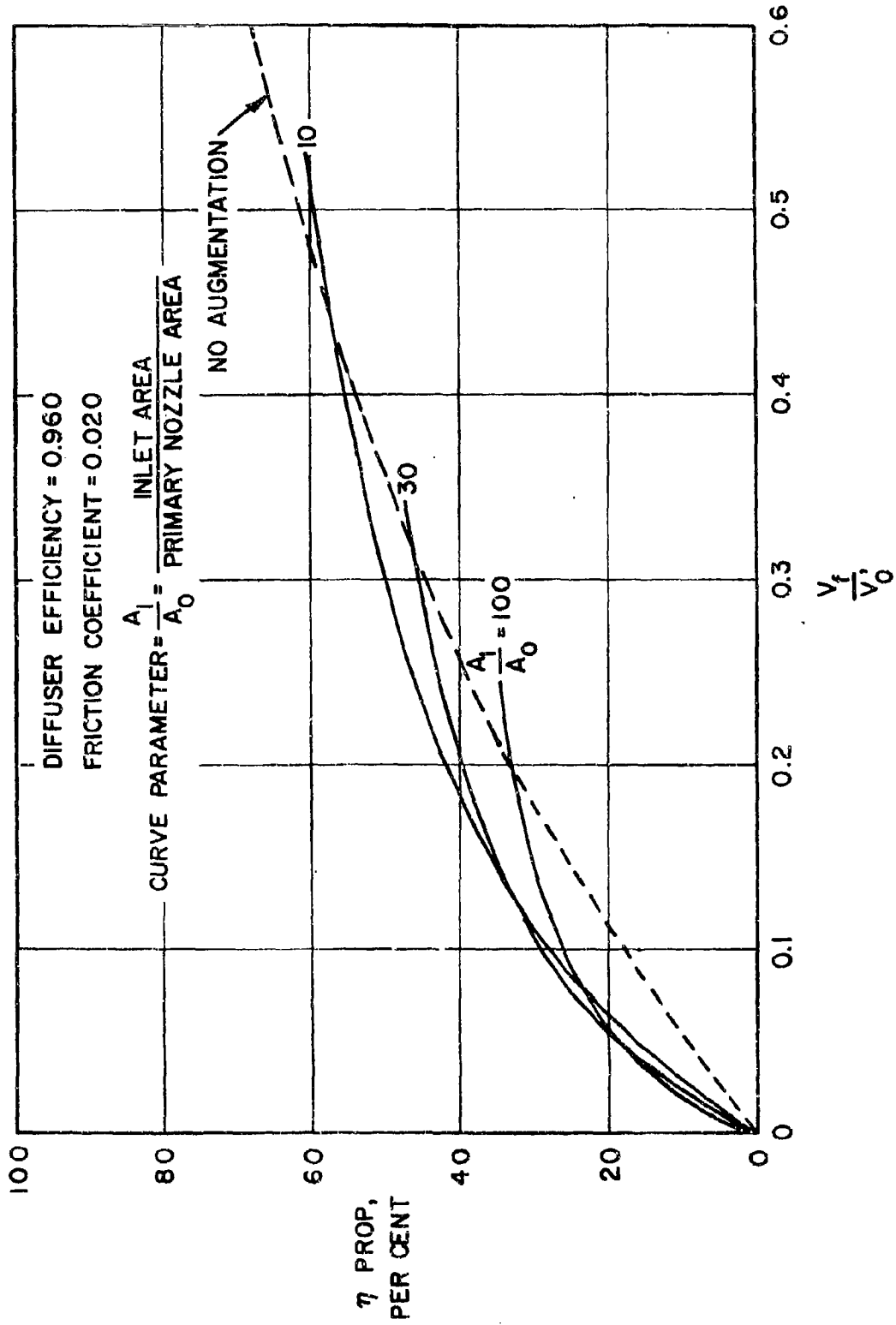


Figure 18

CONFIDENTIAL

PROPULSIVE EFFICIENCY VERSUS FLIGHT SPEED RATIO, V_f/V_0

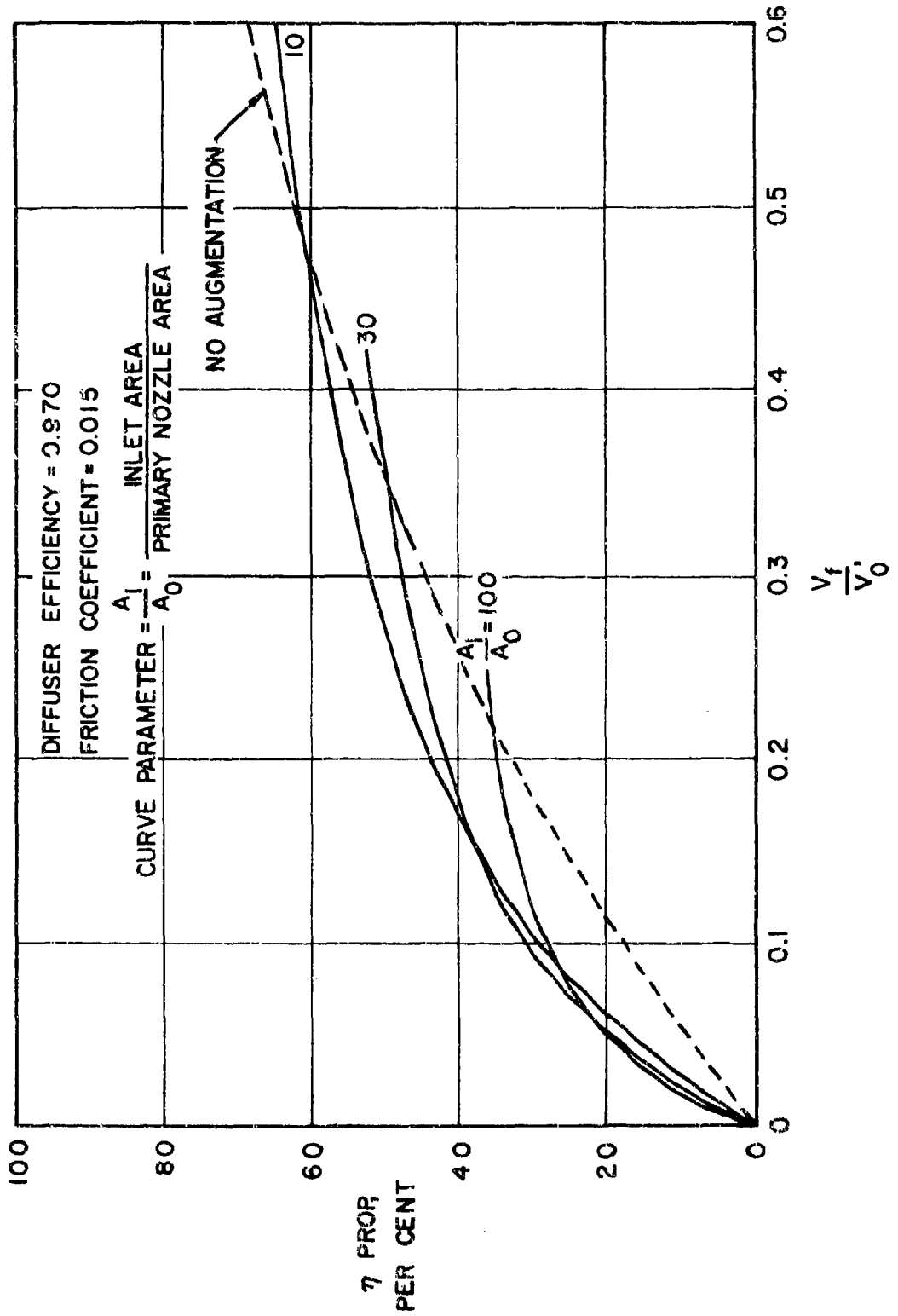


Figure 19

38
CONFIDENTIAL

CONFIDENTIAL

PROPULSIVE EFFICIENCY VERSUS FLIGHT SPEED RATIO. III.

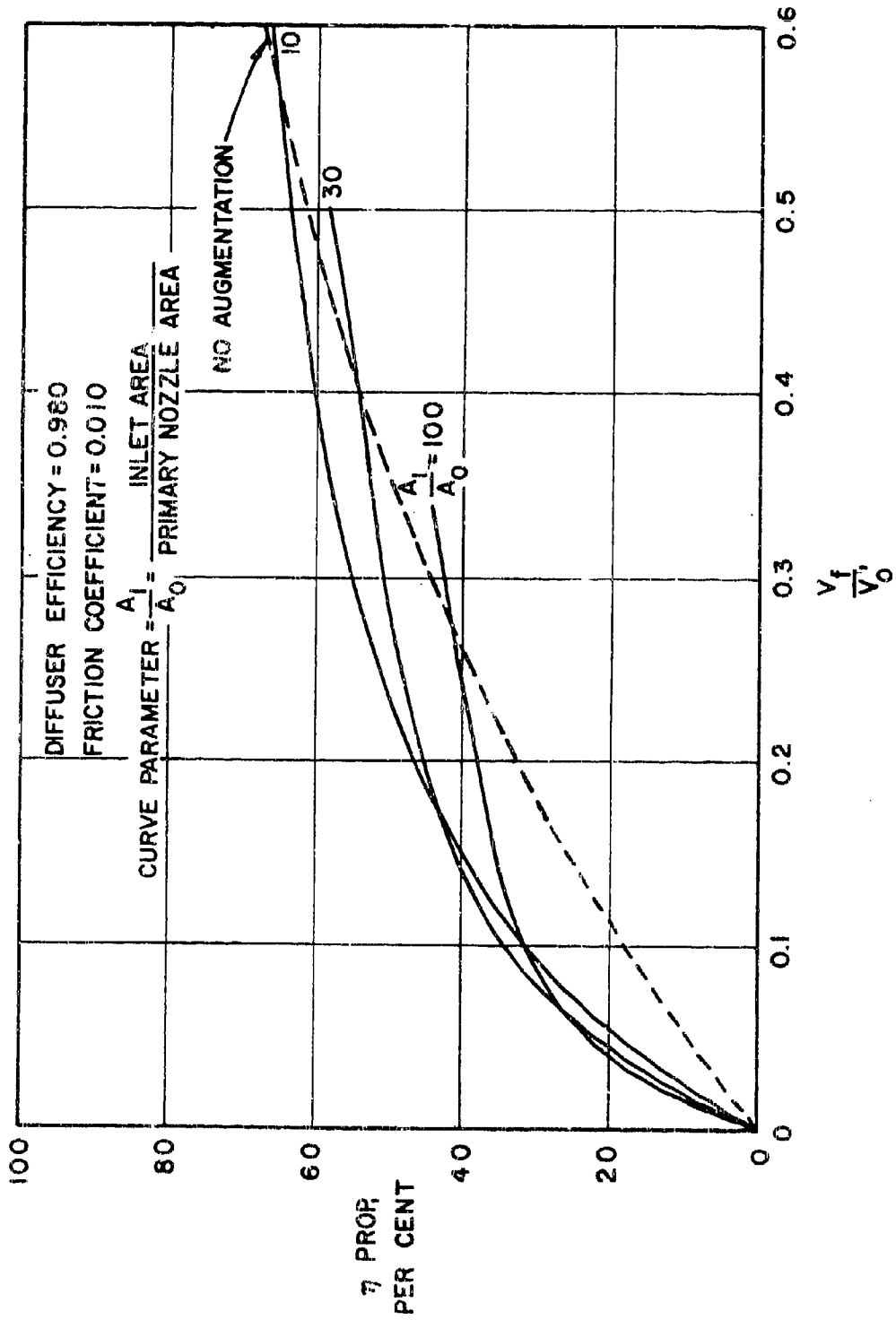
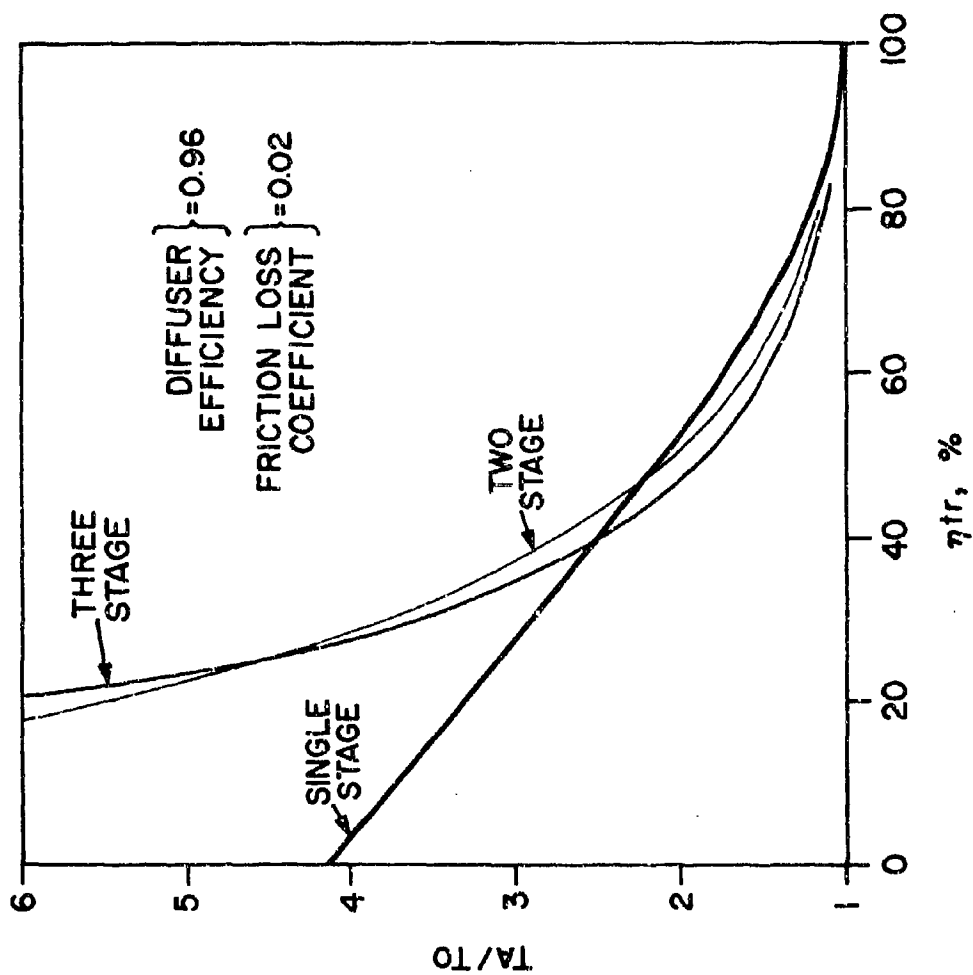
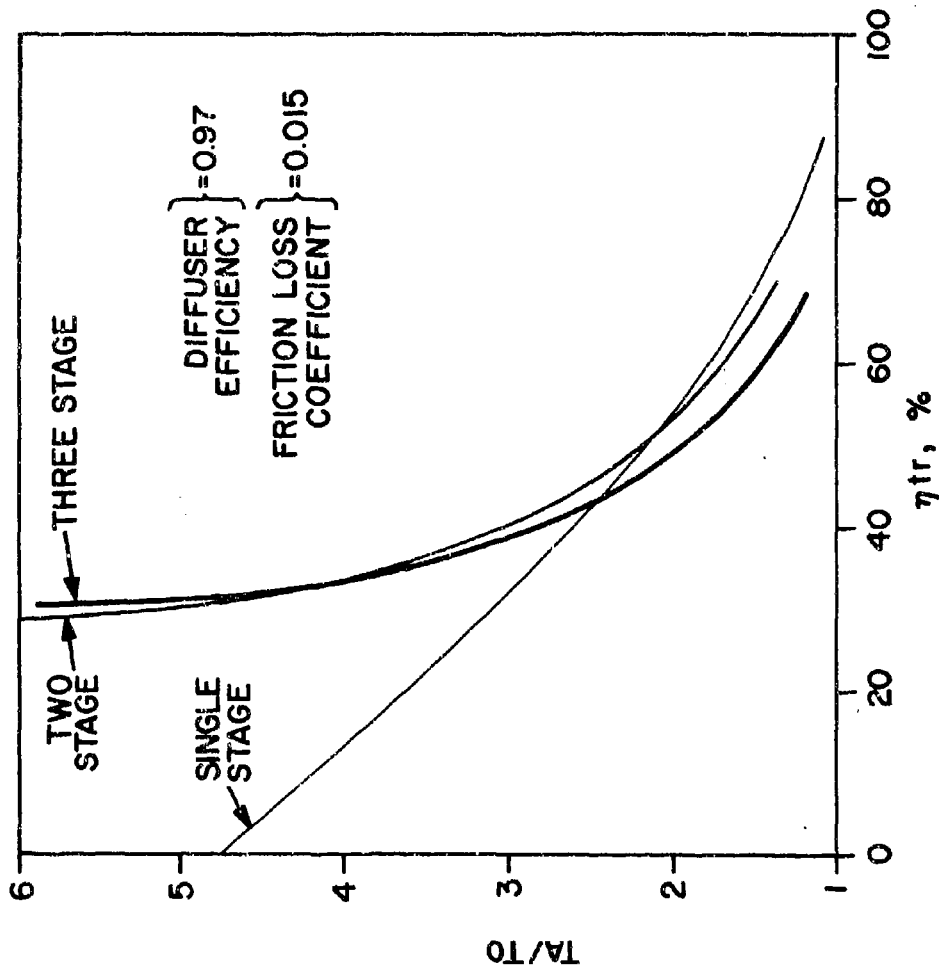


Figure 20



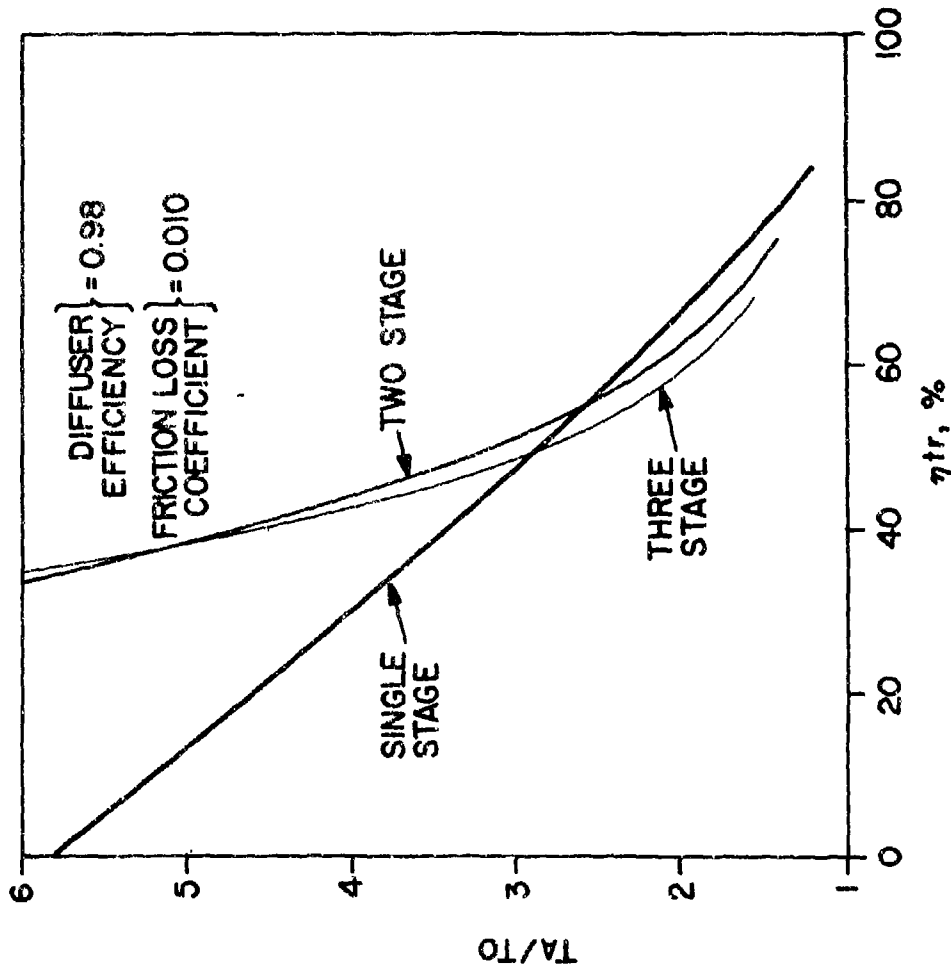
THRUST AUGMENTATION RATIO VS TRANSFER EFFICIENCY FOR 1, 2, AND 3 STAGES.

Figure 21



THRUST AUGMENTATION RATIO VS TRANSFER EFFICIENCY FOR 1, 2, AND 3 STAGES.

Figure 22



THRUST AUGMENTATION RATIO VS TRANSFER EFFICIENCY FOR 1, 2, AND 3 STAGES.

Figure 23

CONFIDENTIAL

THRUST AUGMENTATION RATIO VERSUS TRANSFER
EFFICIENCY. OPTIMUM 2-STAGE. I

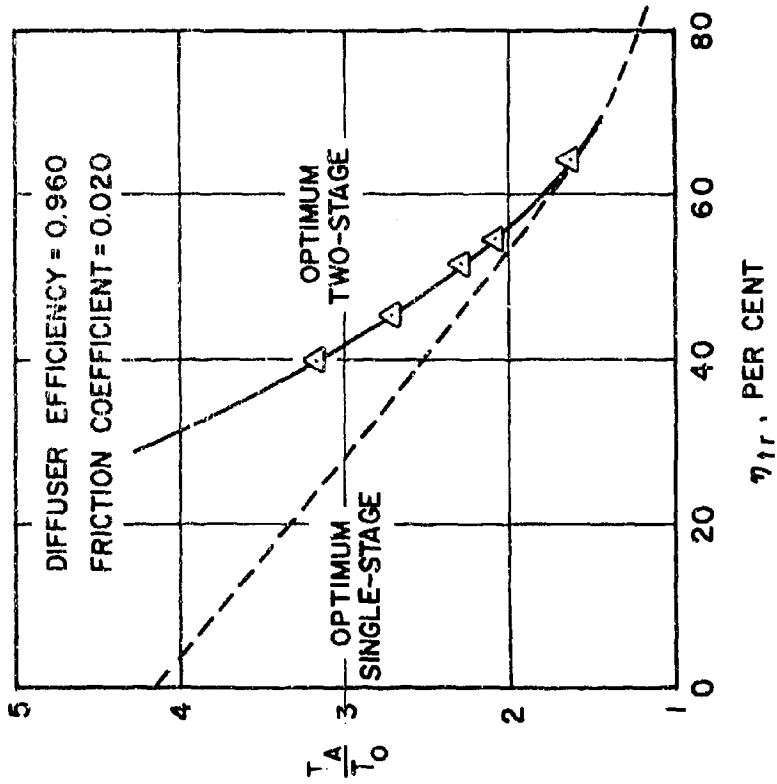


Figure 24

CONFIDENTIAL

THRUST AUGMENTATION RATIO VERSUS TRANSFER EFFICIENCY. OPTIMUM 2-STAGE. II.

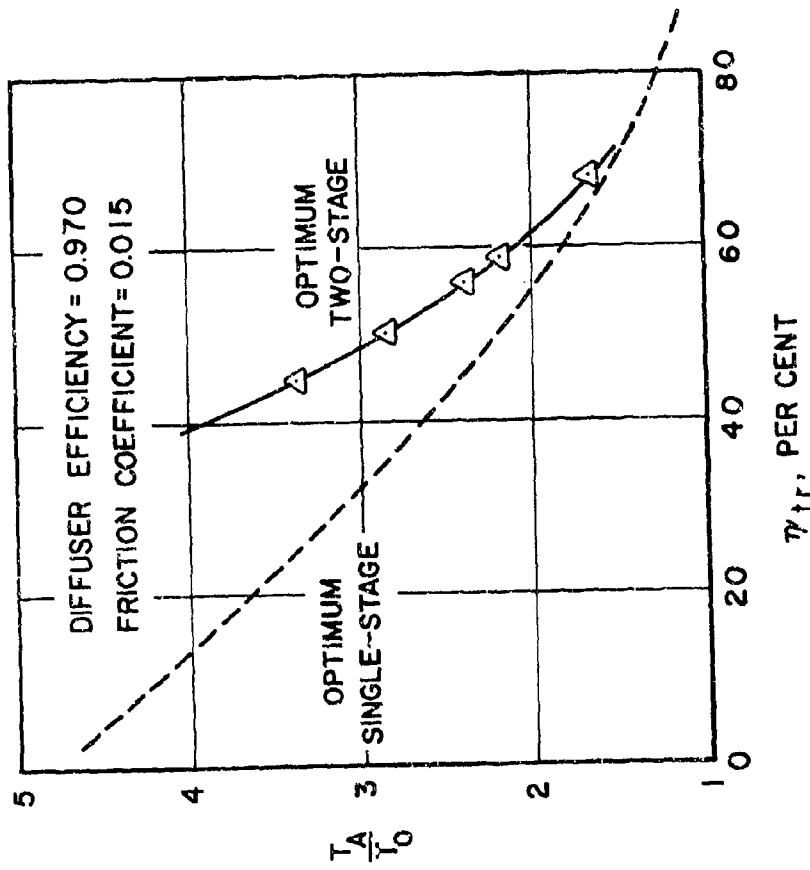


Figure 25

CONFIDENTIAL

THRUST AUGMENTATION RATIO VERSUS TRANSFER EFFICIENCY, OPTIMUM 2-STAGE. II.

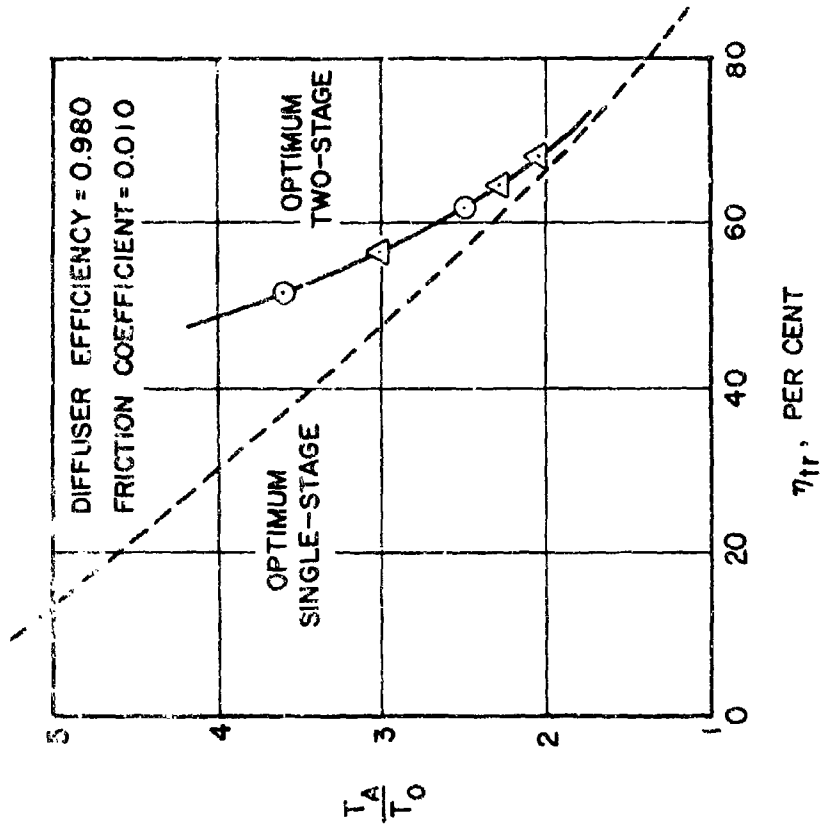
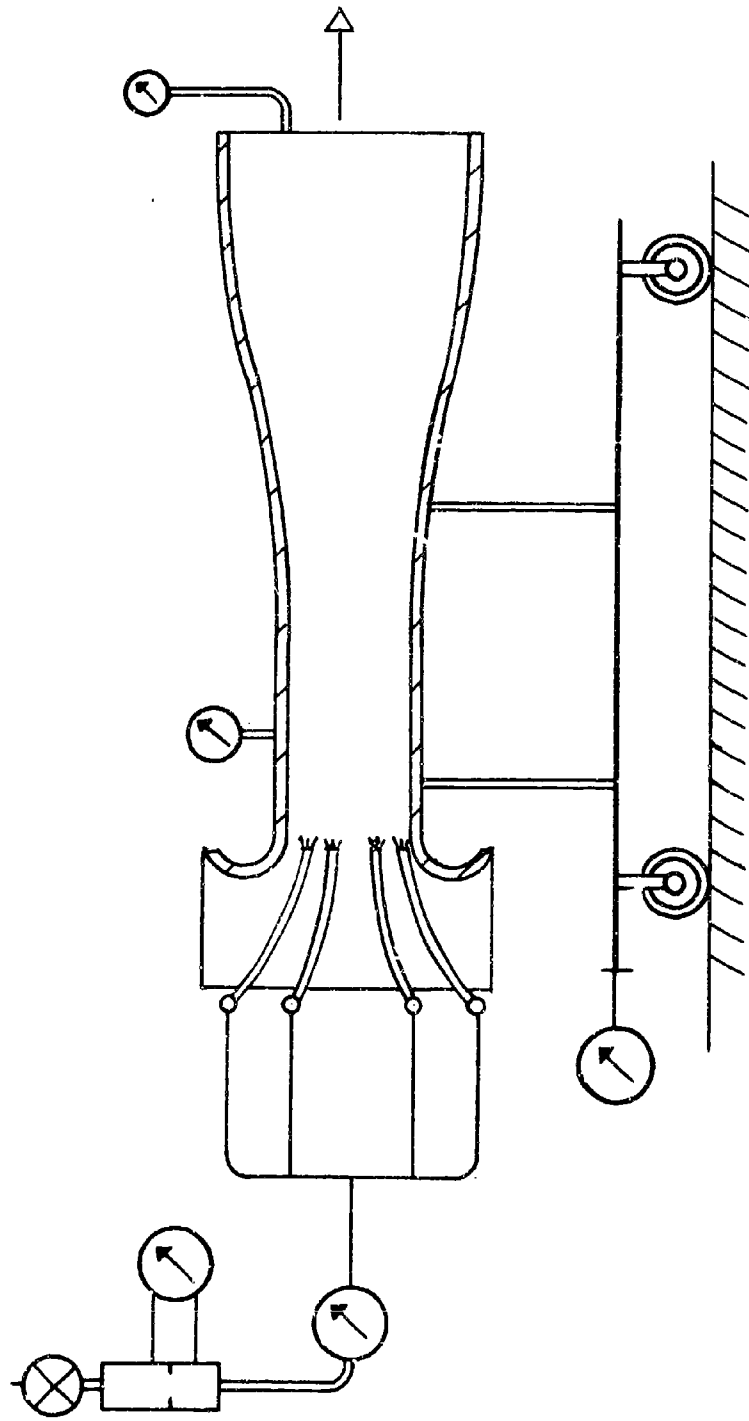


Figure 26

CONFIDENTIAL

THRUST AUGMENTATION TEST RIG



CONFIDENTIAL

CONFIDENTIAL

Figure 27

CONFIDENTIAL

THRUST AUGMENTATION TEST

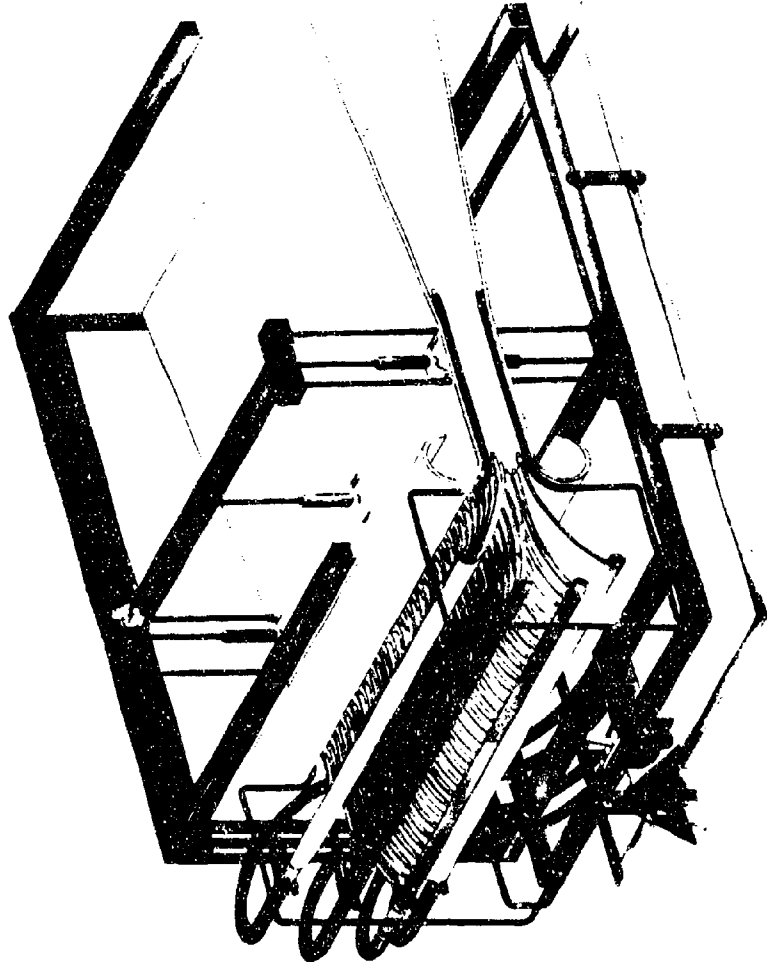
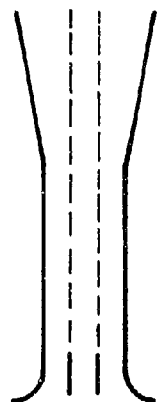


Figure 28

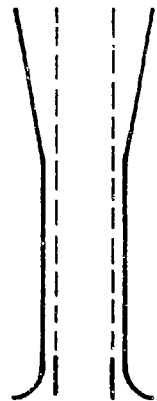
CONFIDENTIAL

MULTIPLE INJECTION, EFFECTS OF PRIMARY NOZZLE LOCATION AND OFF AXIS INCLINATION :

INJECTION PARALLEL TO THE AXIS

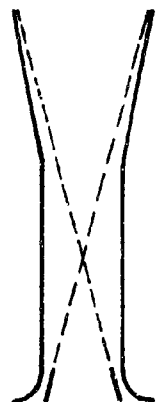


A-2

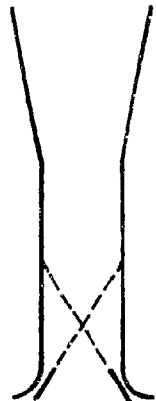


A-1

INJECTION AT INLET BELL MOUTH; (INCLINED TOWARD AXIS)

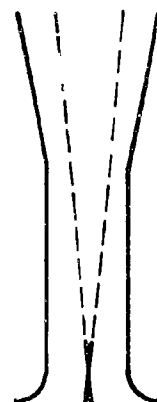


B-2



B-1

MULTI-DIRECTION NOZZLE ROW



C-2



C-1

Figure 29

CONFIDENTIAL

EXPERIMENTAL MEASUREMENT OF THRUST AUGMENTATION RATIO VERSUS MANIFOLD PRESSURE HEAD

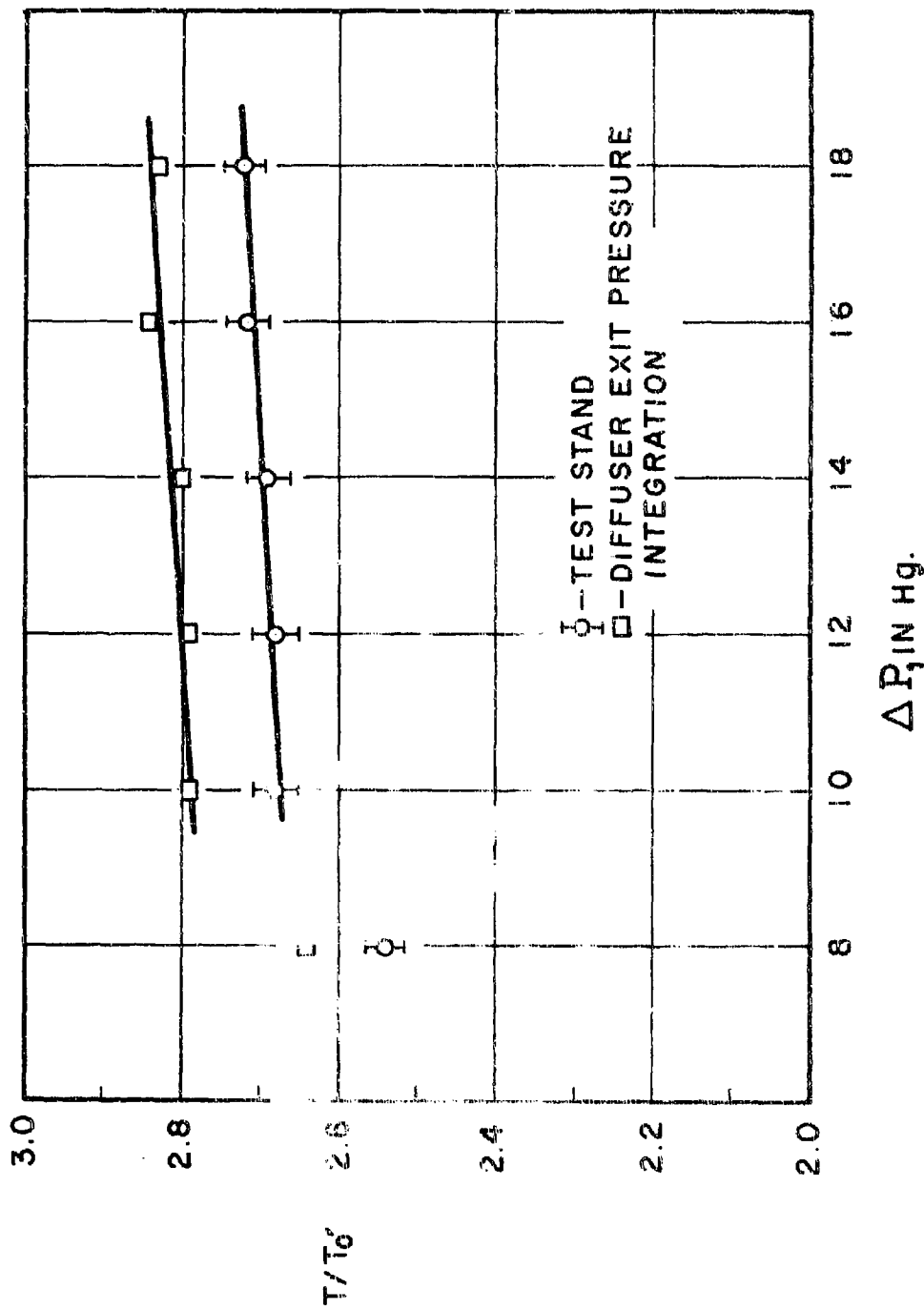


Figure 30

CONFIDENTIAL

CONFIDENTIAL

EXPERIMENTAL DATA SHOWING INFLUENCE OF PRIMARY NOZZLE INCLINATION

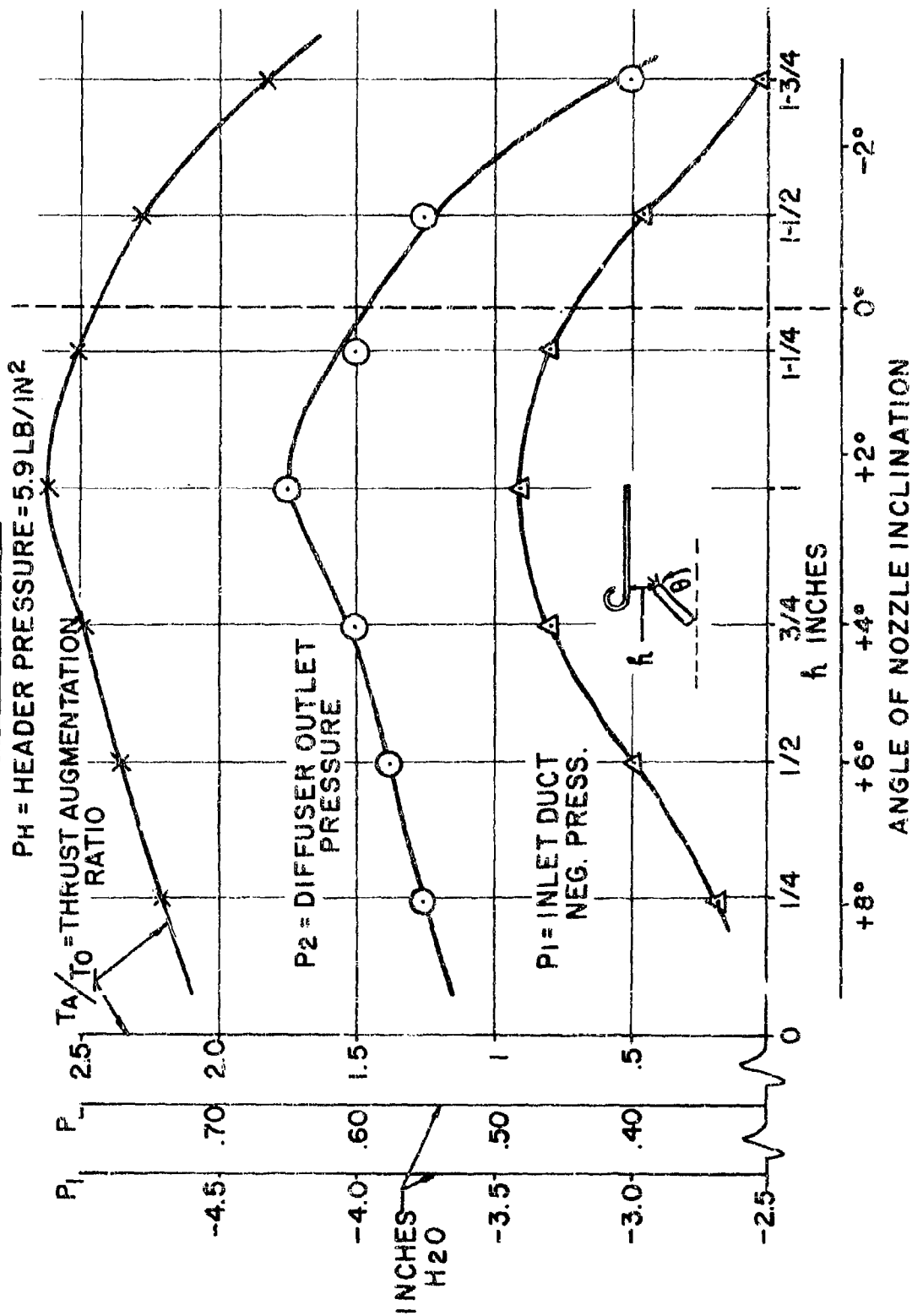


Figure 31

Thrust Augmentation Process For Air Breathing V/STOL Aircraft

CONFIDENTIAL

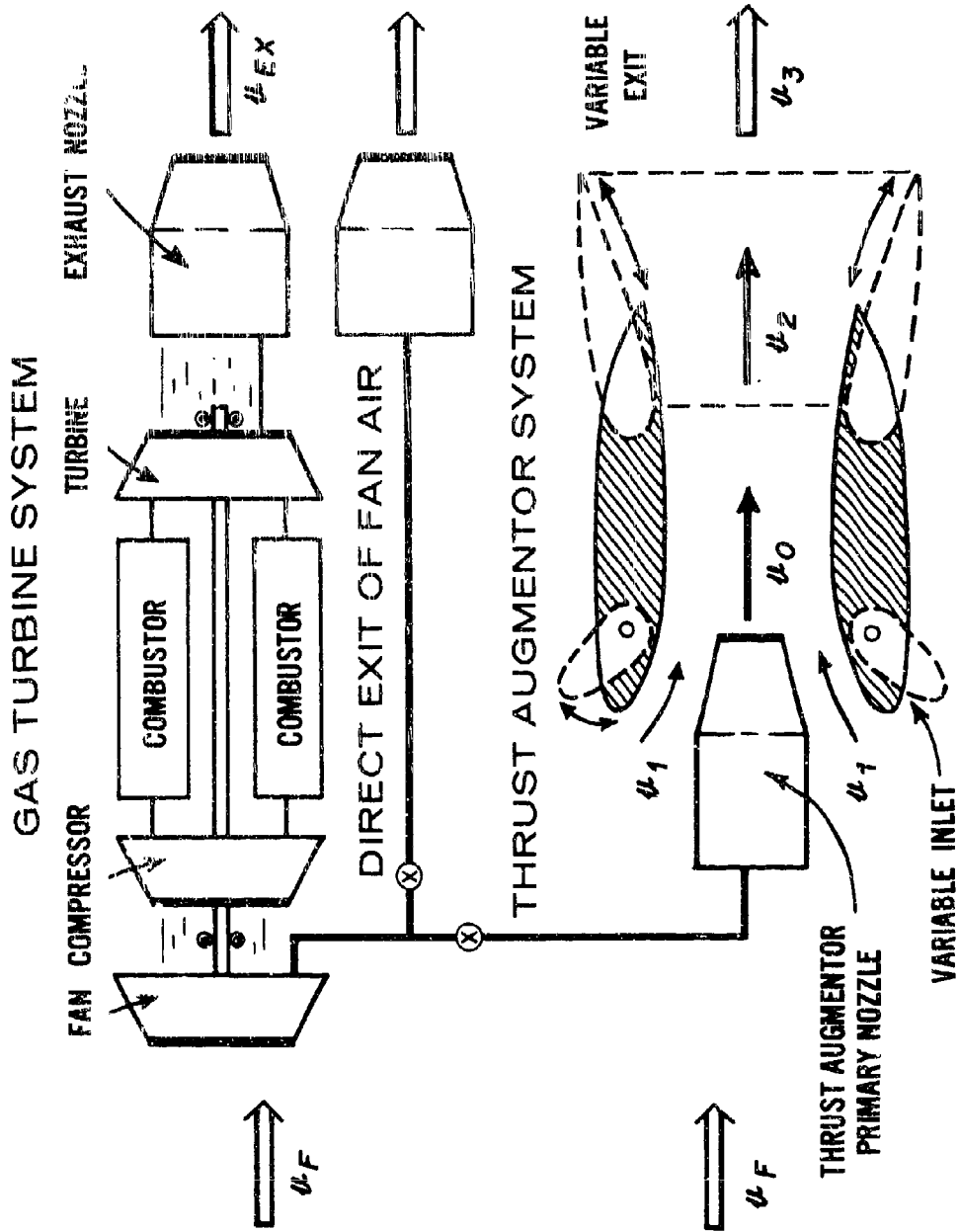


Figure 32

CONFIDENTIAL

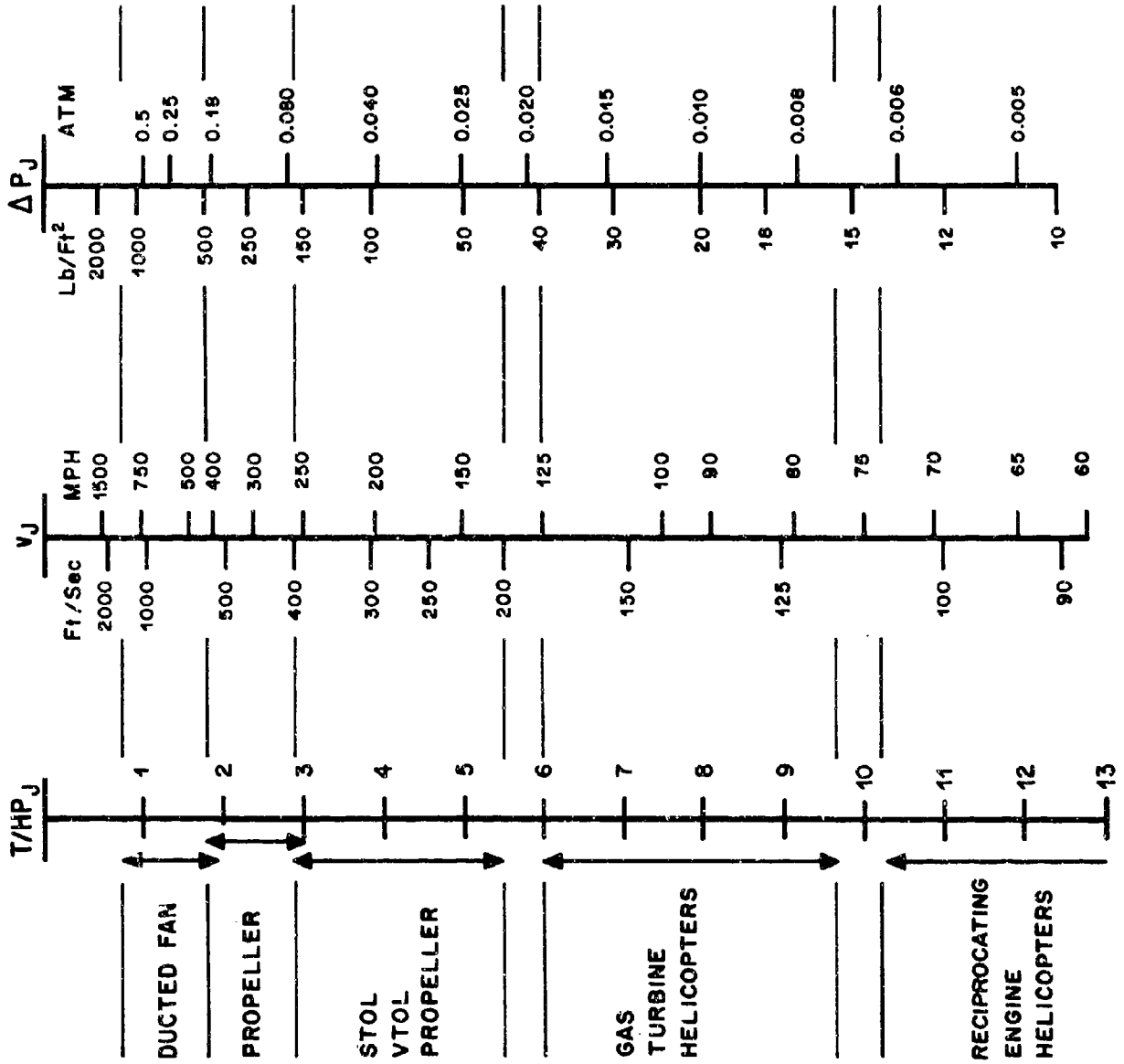


Figure 33 V/STOL PROPULSION CHART

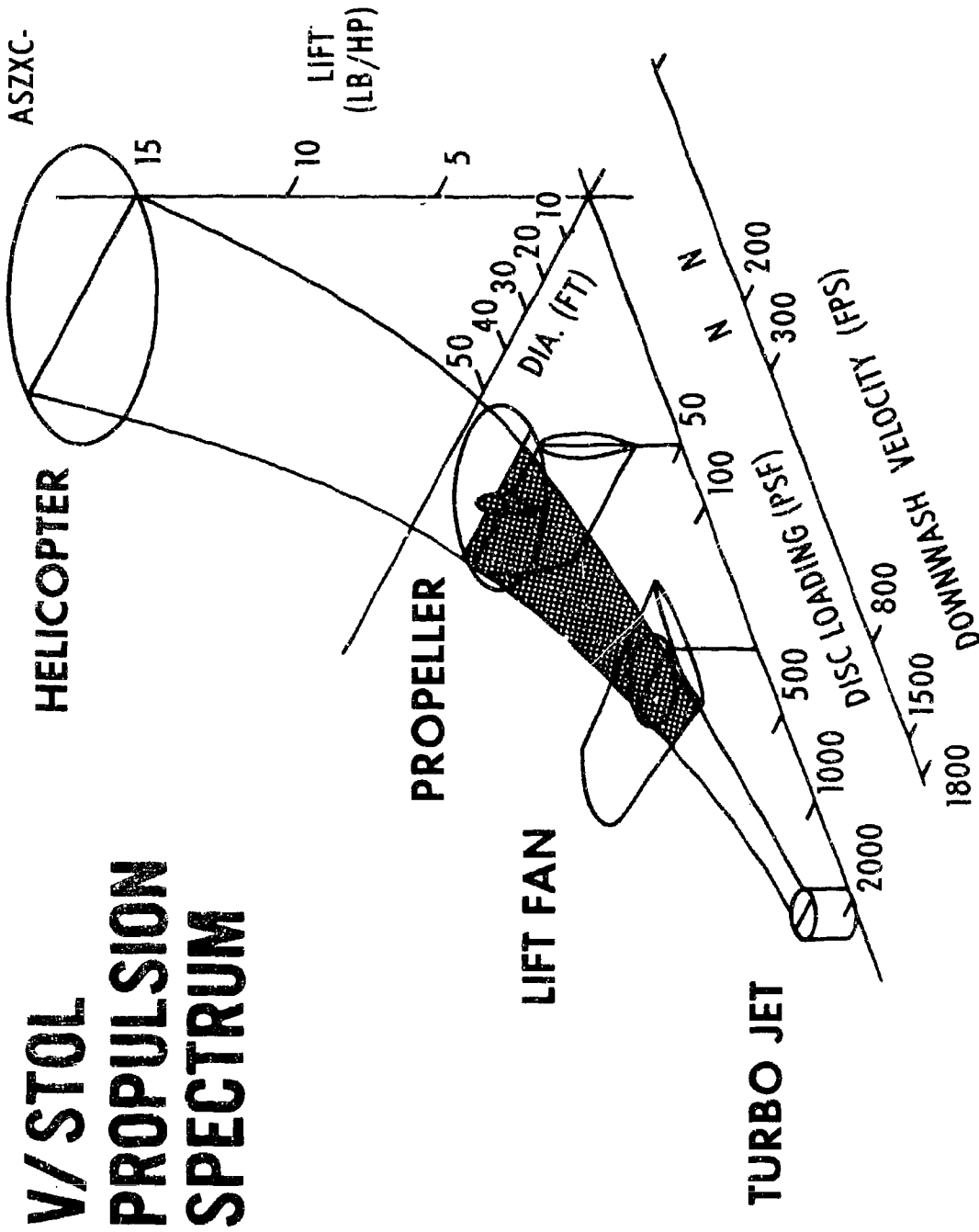


Figure 34

CONFIDENTIAL

RELATIONSHIPS BETWEEN THRUST AUGMENTATION PERFORMANCE
AND CHARACTERISTIC AREA RATIOS

A_w = WING AREA; A_{Di} = INITIAL DUCT AREA

A_o = PRIMARY NOZZLE AREA; A_1 = ASPIRED AIR INLET AREA;

$$A_2 = A_1 + A_o$$

A_3 = DIFFUSER EXIT AREA;

$$\frac{A_3}{A_w} = 3.5 \cdot 10^{-4} \times \text{WINGLOADING} \times \left(\frac{\text{LIFT THRUST}}{\text{FAN POWER}} \right)^2 \times \left(\frac{1}{\eta_{tr}} \right)^2; \langle \text{Ft ; lbs; HP} \rangle$$

$$\frac{\text{LIFT THRUST}}{\text{FAN POWER}} = \text{THRUST AUGMENTATION RATIO} \times \frac{\text{FAN THRUST}}{\text{FAN POWER}} ;$$

$$A_{Di} \geq 3 A_o;$$

$$\frac{A_{Di}}{A_w} = 3 \frac{A_o}{A_1} \cdot \frac{A_1}{A_1 \times A_o} \cdot \frac{A_2}{A_3} \cdot \frac{A_3}{A_w}$$

Figure 35

DIFFUSER EXIT TO WING AREA RATIO, A_D/A_W , VERSUS AUGMENTED
THRUST PER FAN HORSEPOWER, T/HP_{fan}
CURVE PARAMETER = TRANSFER EFFICIENCY, η_{tr}

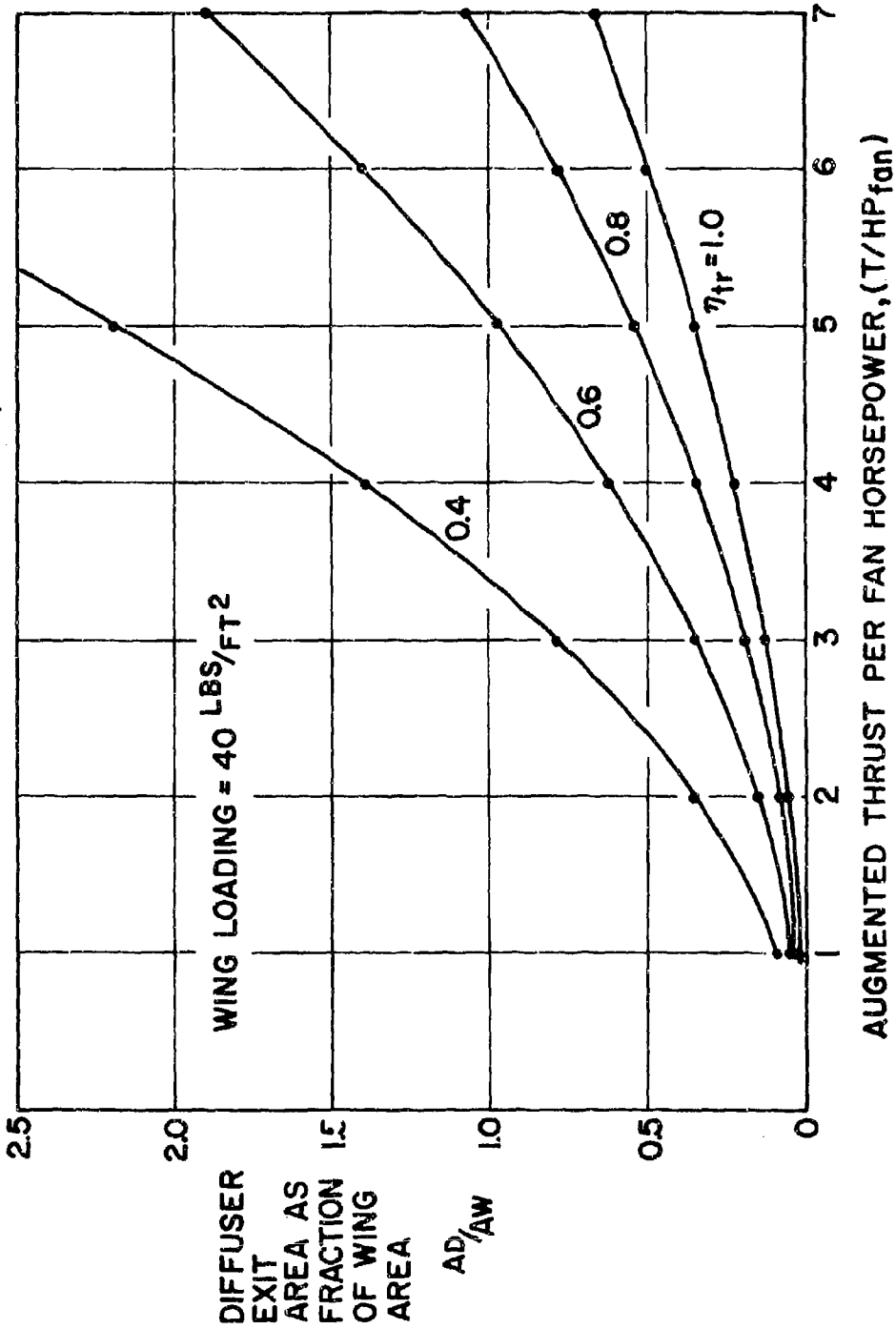


Figure 36

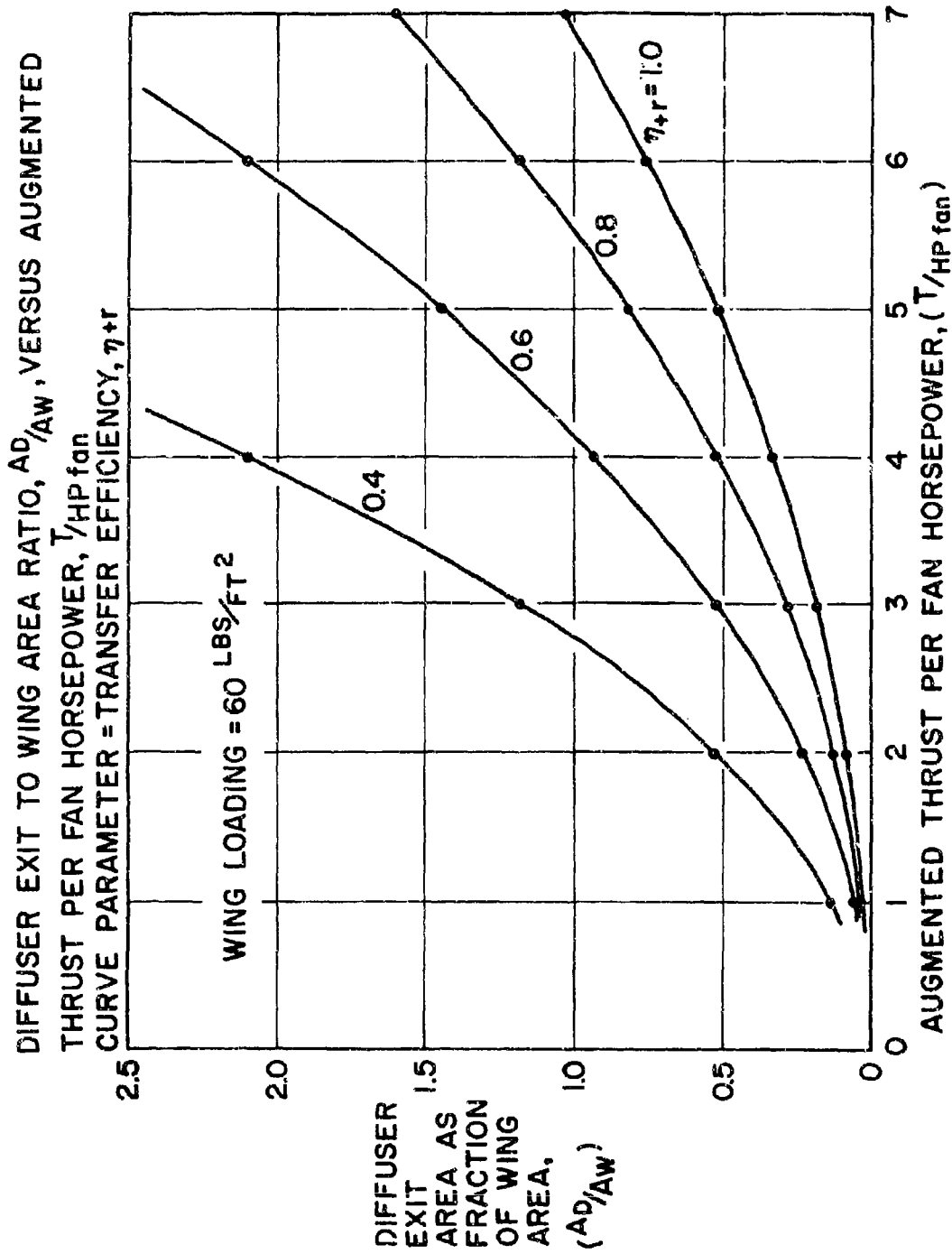


Figure 37

BASIC AIRCRAFT TYPES EMPLOYING THRUST AUGMENTATION

- I. VERTICAL EJECTOR CONFIGURATIONS WING CENTER; FUSELAGE
- II. HORIZONTAL EJECTOR CONFIGURATIONS
 - A: ENERGY TRANSFER TO UNDISTURBED FLOW
 - THRUST AUGMENTATION ON SUCTION OR PRESSURE SIDE
 - DIFFUSER AREA CONTROL UNCOUPLED OR COUPLED WITH THRUST VECTORING FLAP
 - B: ENERGY TRANSFER TO VEHICLE BOUNDARY LAYER SHROUDED OR UNSHROUDED CONFIGURATION
 - C: HYBRIDS OF (A) AND (B)

SCHEMATIC OF SUPERSONIC VTOL AIRCRAFT WITH THRUST AUGMENTATION

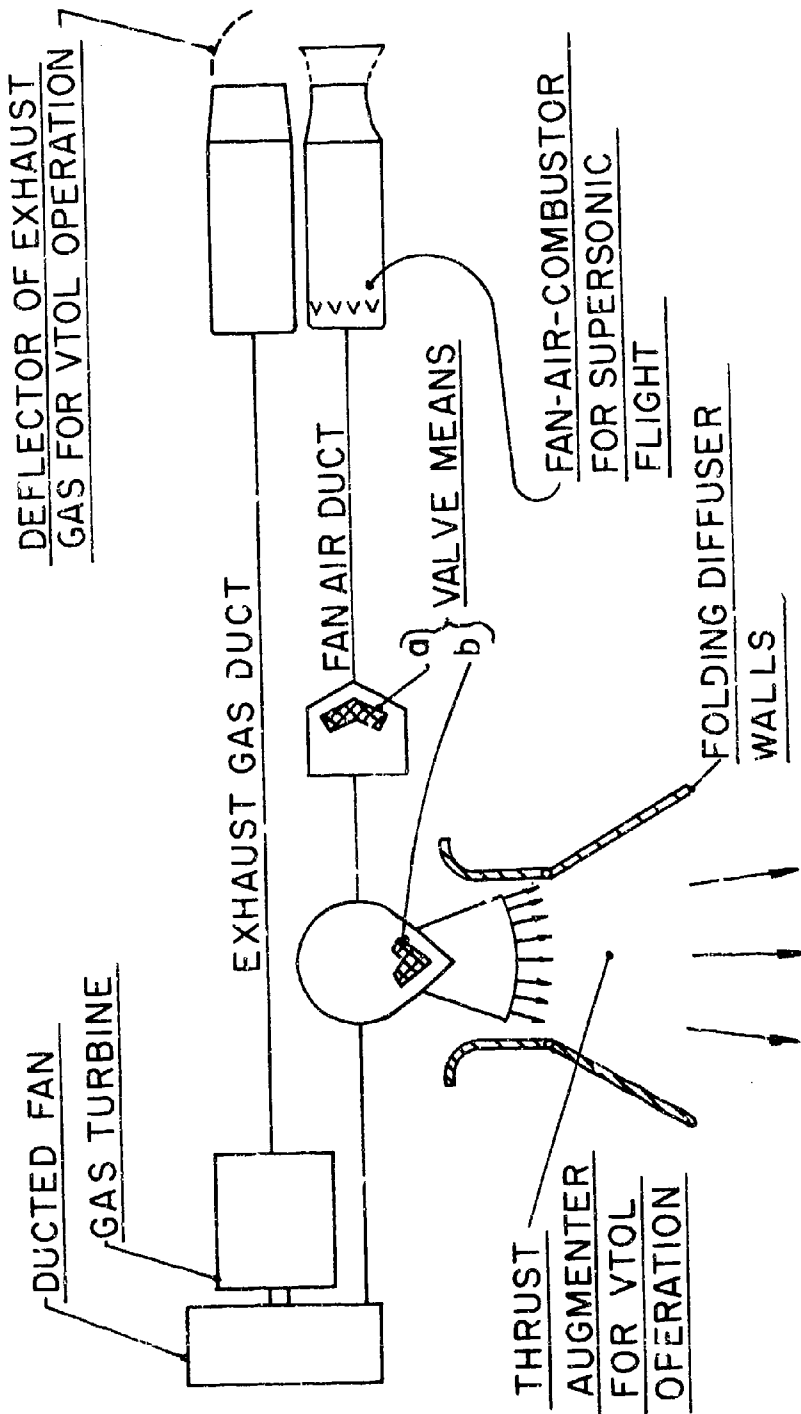


Figure 39

CONFIDENTIAL

SCHEMATIC VIEW OF SUPERSONIC VTOL AIRCRAFT
WITH CENTRALLY LOCATED VERTICAL THRUST
AUGMENTORS:(COLD ENGINE BYPASS AIR IS
EMPLOYED AS DRIVER GAS)

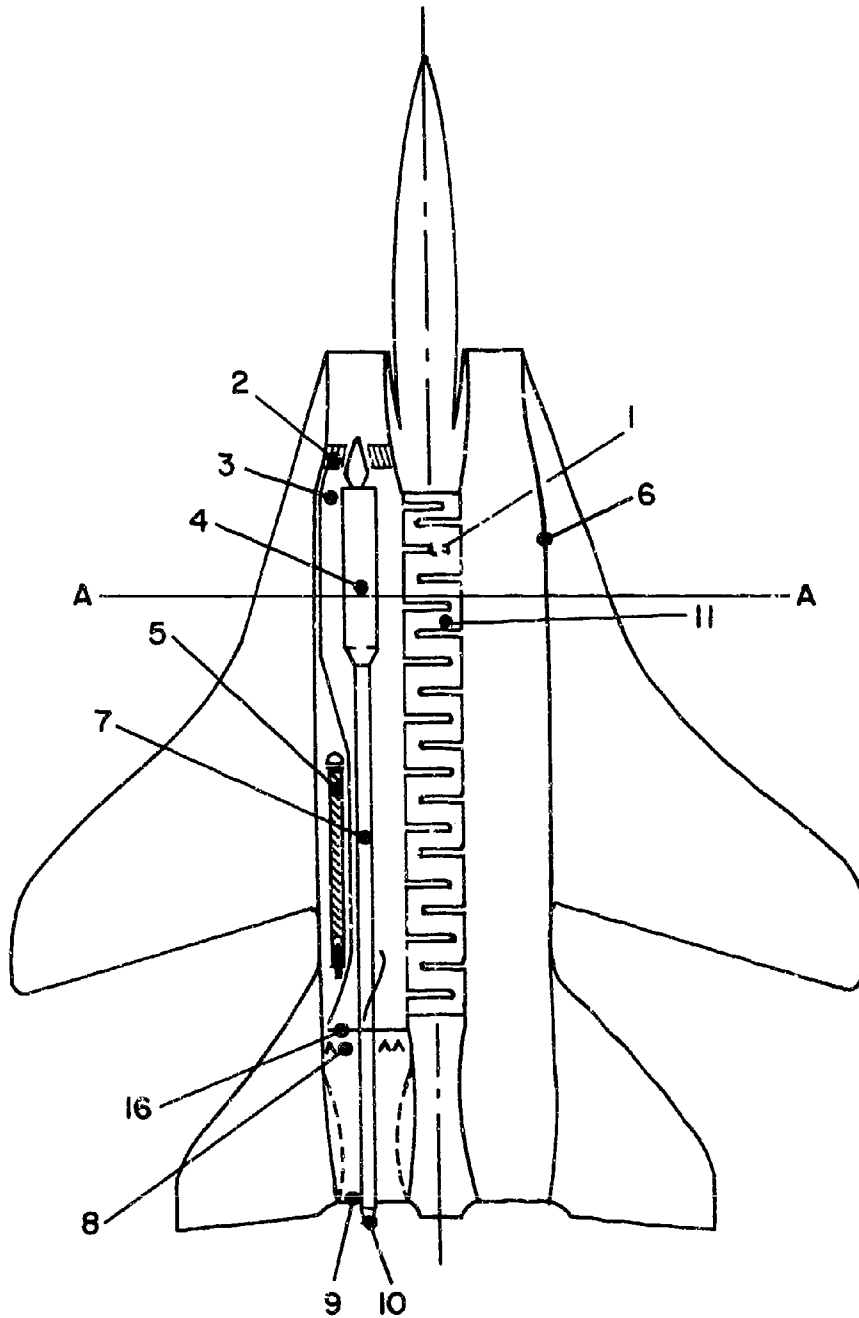
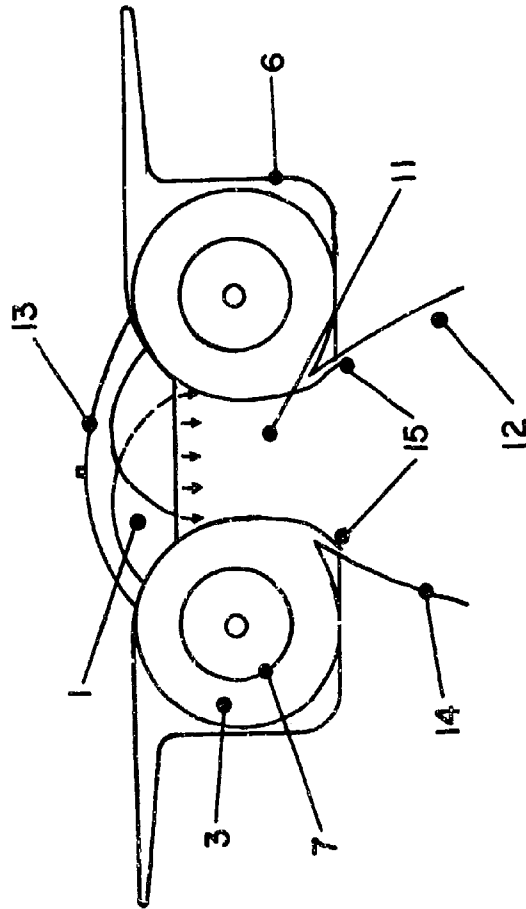


Figure 40

CONFIDENTIAL

CONFIDENTIAL.



VIEW A-A

Figure 41

PROPULSIVE WING

- SUCTION SIDE OF WING
- DIFFUSER AREA CONTROL INDEPENDENT OF THRUST VECTORING

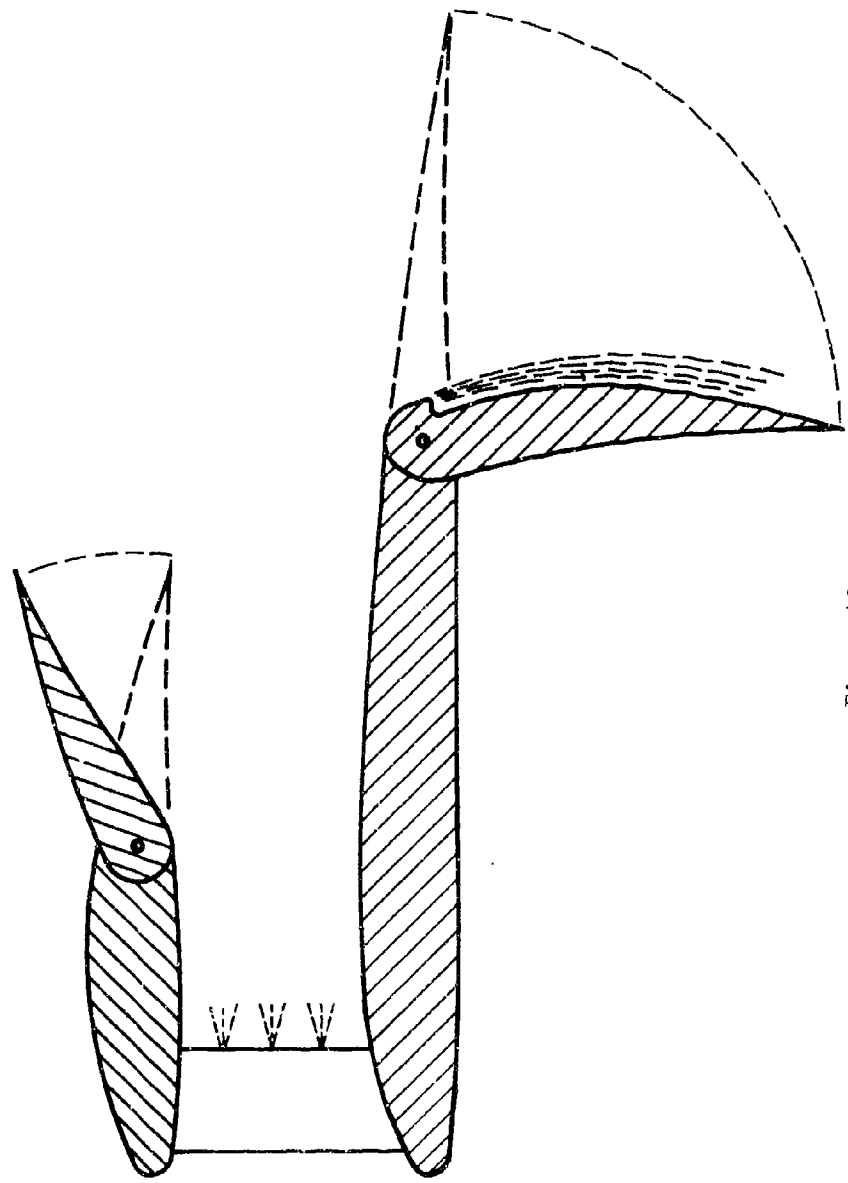
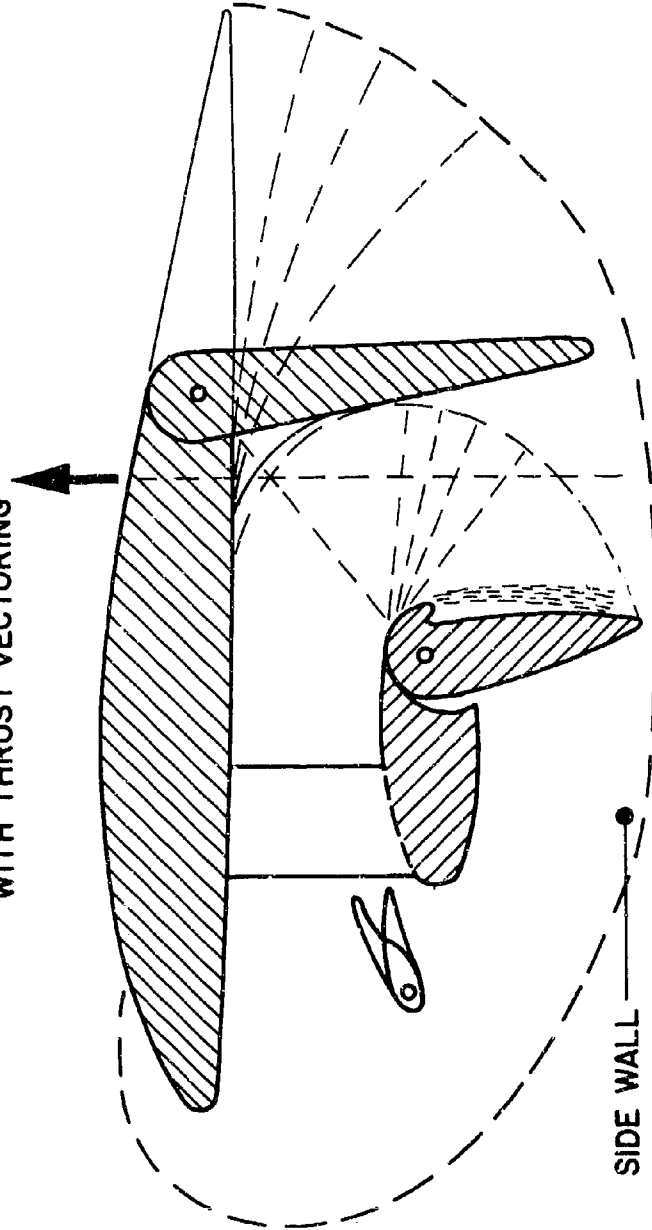


Figure 42

PROPULSIVE WING (VERTICAL THRUST)

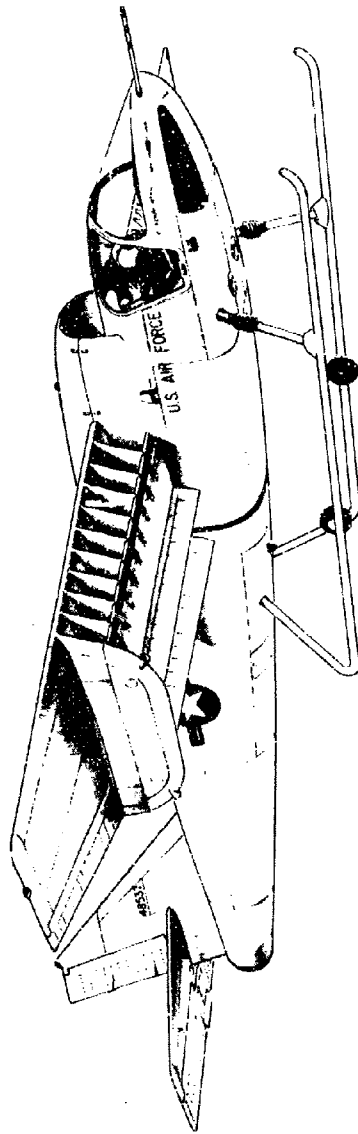
- ENERGY TRANSFER TO UNDISTURBED AIR
- PRESSURE SIDE OF WING
- DIFFUSER AREA CONTROL COUPLED WITH THRUST VECTORING



SIDE WALL

Figure 4.3

CONFIDENTIAL



58

CONFIDENTIAL

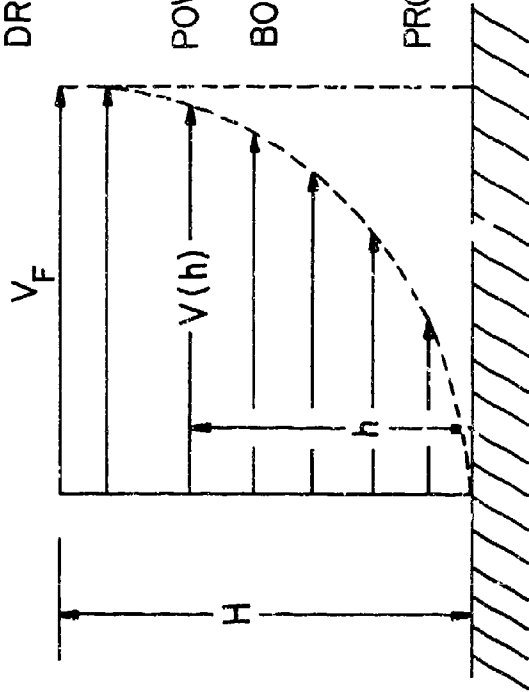
PROPULSION BY ACCELERATION OF BOUNDARY LAYER:

DRAG: $D = \rho \int_0^H (V_F - V(h)) V(h) dh$

POWER REQUIRED FOR ACCELERATION OF

BOUNDARY LAYER: $L_R = \frac{\rho}{2} \int_0^H (V_F^2 - V^2(h)) V(h) dh$

PROPULSIVE EFFICIENCY: $\eta_{PROP} = \frac{D \cdot V_F}{L_R}$



FOR $V(h) = V_F \left(\frac{h}{H}\right)^{\frac{1}{n}}$

$\eta_{PROP} = \frac{n+3}{n+2}$

Figure 45

SHROUDED WING CONFIGURATION FOR FLUIDDYNAMIC
ENERGY TRANSFER TO BOUNDARY LAYER

TRANSSONIC LONG RANGE STOL TRANSPORT

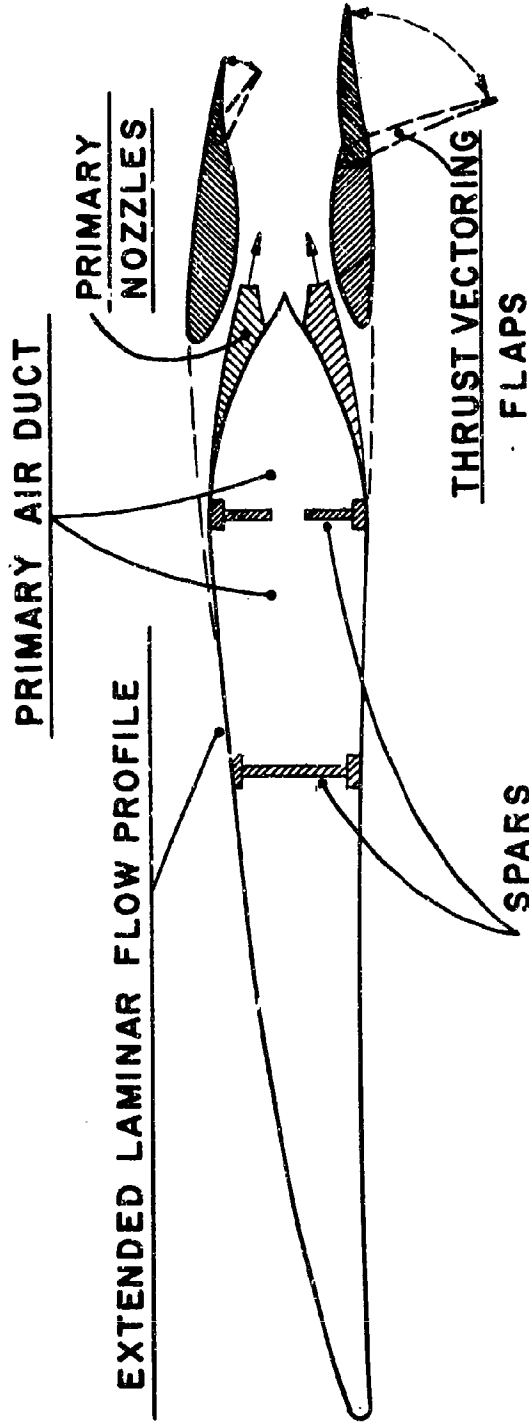


Figure 46

INCREASE OF TOTAL MOMENTUM
BY BOUNDARY LAYER ACCELERATION

<SHROUDED CONFIGURATION>

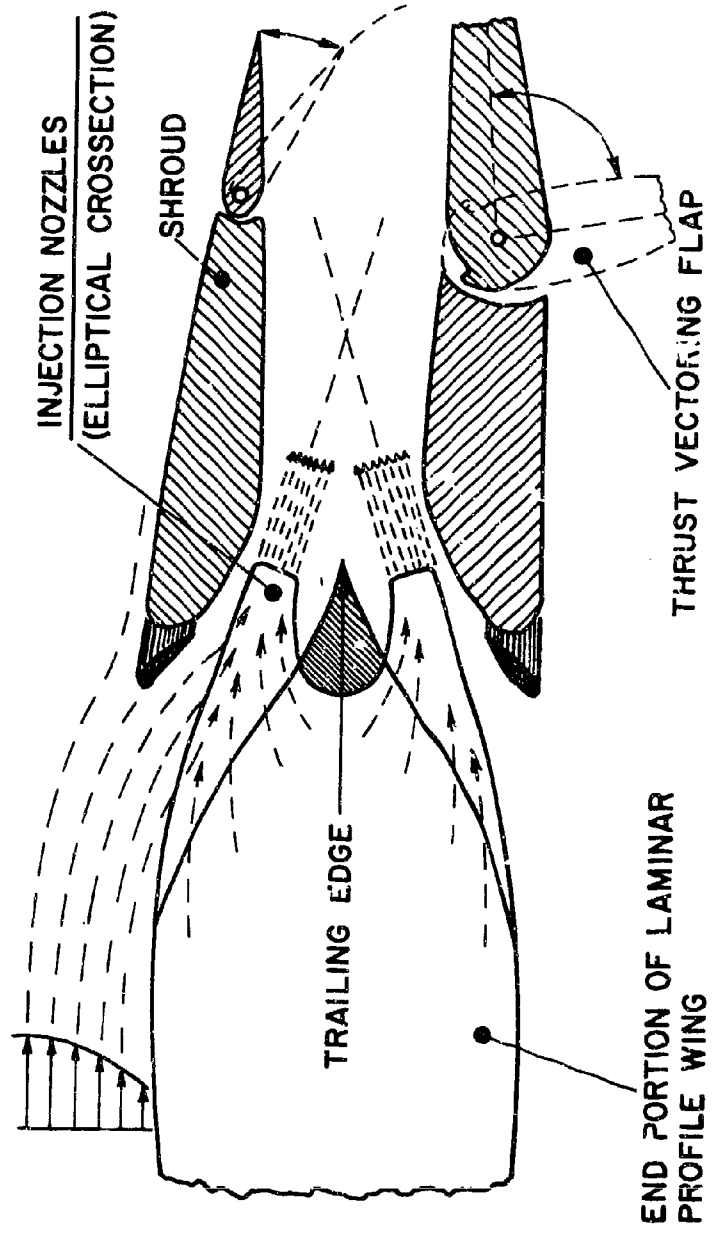


Figure 47

NON SHROUDED WING CONFIGURATION FOR FLUIDYNAMIC
ENERGY TRANSFER TO BOUNDARY LAYER

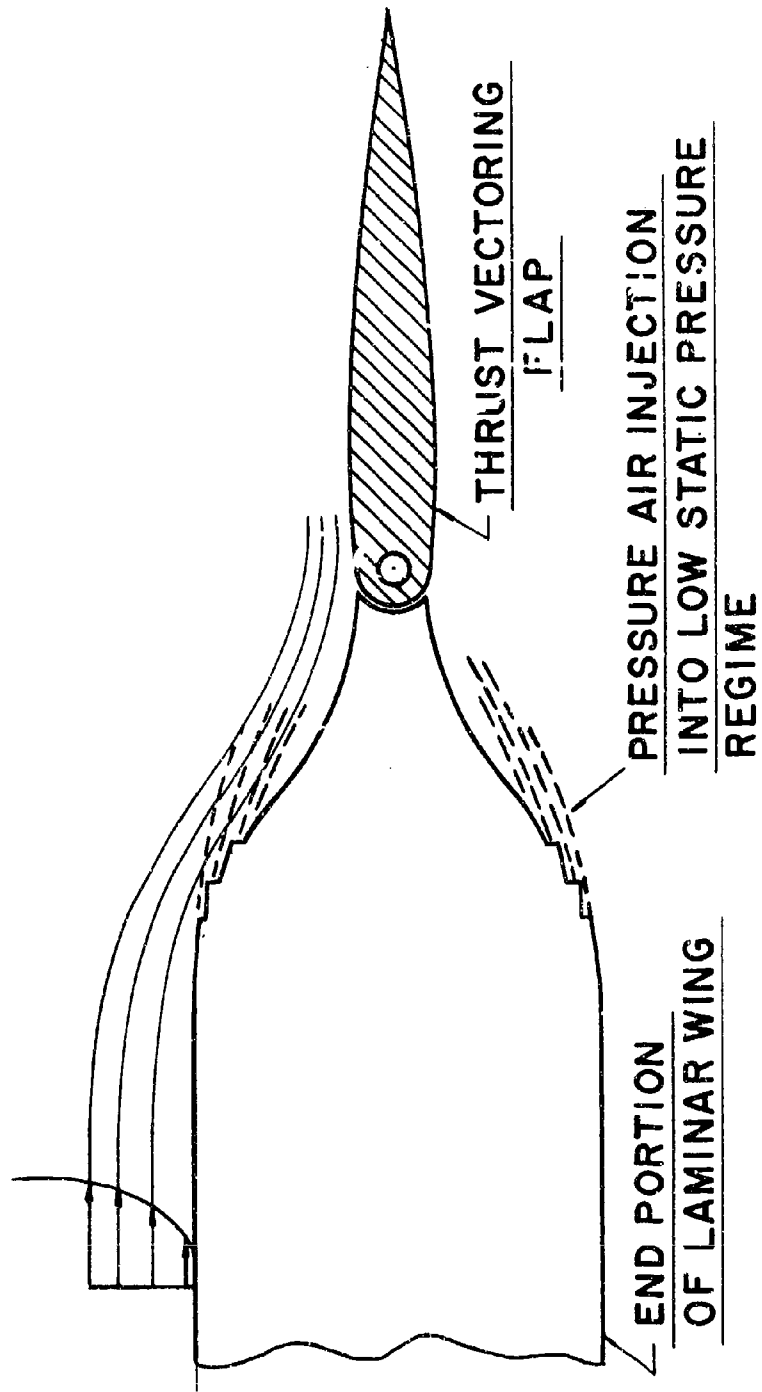
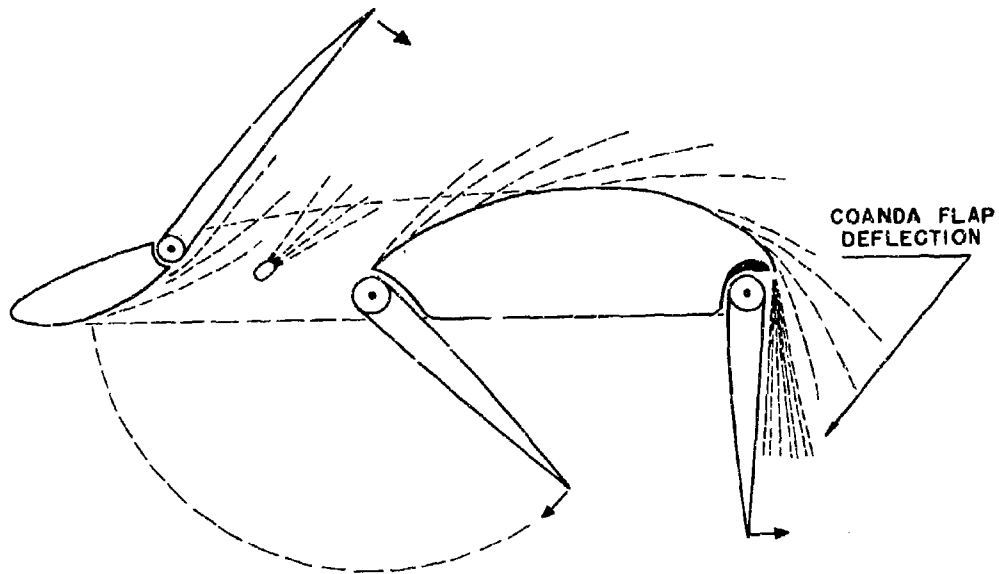


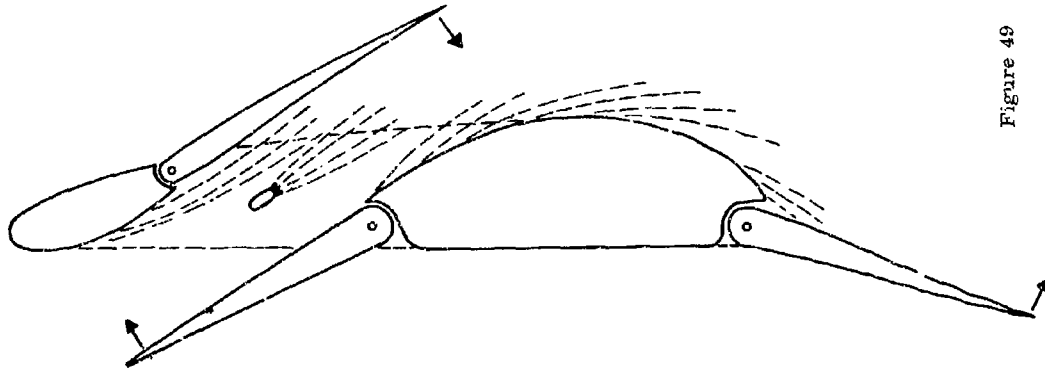
Figure 48

CONFIDENTIAL

CONFIDENTIAL



TYPE I: THRUST AUGMENTATION UNDER STATIC CONDITIONS, EJECTOR DISCHARGING TO SUCTION SIDE OF WING.



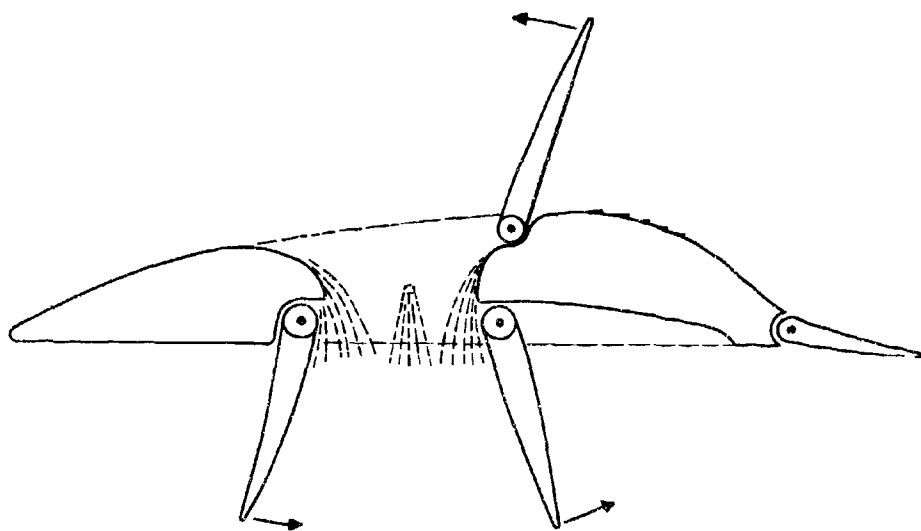
TYPE I: THRUST AUGMENTATION DURING STOL CONDITIONS OR DURING TRANSITION TO AERODYNAMICALLY SUSTAINED FLIGHT.



TYPE I: THRUST AUGMENTATION IN FLIGHT BY BOUNDARY LAYER ACCELERATION (PRIMARY AIR INJECTION AND MIXING IN REGIME OF LOWEST STATIC PRESSURE).

CONFIDENTIAL

CONFIDENTIAL



TYPE 2: SIMILAR TO TYPE 1, BUT THRUST AUGMENTATION UNDER STATIC CONDITIONS HAS EJECTOR DISCHARGING TO PRESSURE SIDE OF WING.

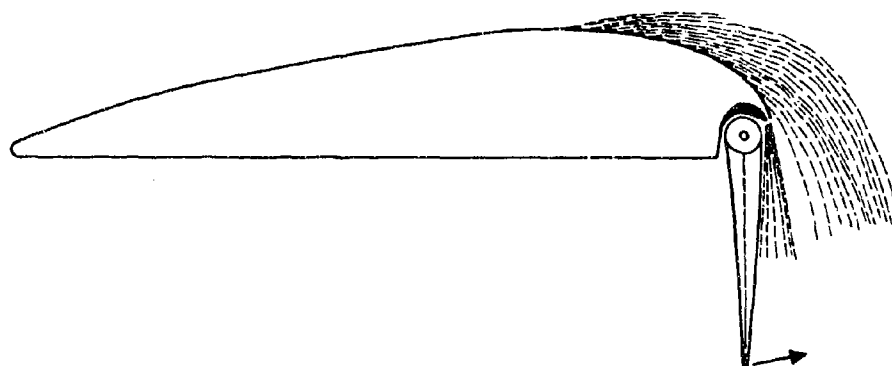
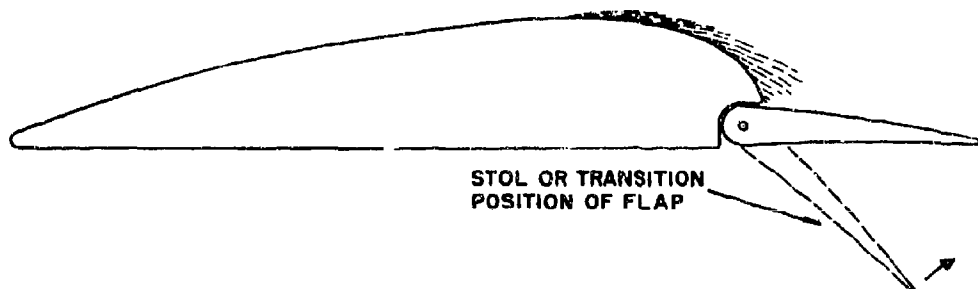


Figure 50

TYPE 3: EXTERNAL FLOW THRUST AUGMENTATION UNDER VTOL CONDITIONS, INDIVIDUAL JET NOZZLES AND COANDA FLAP DEFLECTION.



STOL OR TRANSITION
POSITION OF FLAP

TYPE 3: THRUST AUGMENTATION IN FLIGHT BY BOUNDARY LAYER ACCELERATION (PRIMARY AIR INJECTION AND MIXING IN REGIME OF LOWEST STATIC PRESSURE).

CONFIDENTIAL

CONFIDENTIAL

FUNDAMENTAL RESEARCH ON THRUST AUGMENTATION

- LENGTH REDUCTION
- **MIXING**
 - EFFECTS OF INJECTION METHOD
- **BOUNDARY LAYER PHENOMENA**
- **FLOW MODELS:**
 - INCOMPRESSIBLE AND COMPRESSIBLE
 - ONE-, TWO-, AND THREE-DIMENSIONAL FLOWS
 - INTERNAL (SHROUDED); EXTERNAL (UNSHROUDED)
 - SINGLE-STAGE, MULTI-STAGE PROCESSES
 - ENERGY TRANSFER TO:
 - UNDISTURBED FLOW
 - VEHICLE BOUNDARY LAYER

Figure 51

ENGINEERING RESEARCH ON THRUST AUGMENTATION FOR V/STOL

- THRUST VECTORING METHODS
- INLET CONFIGURATIONS COMPATIBLE WITH STILLSTAND AND HIGH-SPEED FLIGHT
- WIND TUNNEL INVESTIGATIONS
- ENGINE CONSIDERATIONS
- PROPULSION SYSTEM — AIRFRAME INTEGRATION
- FLIGHT DYNAMIC CHARACTERISTICS
- DEMONSTRATOR AIRCRAFT
- NOVEL AIRCRAFT SYSTEM CONCEPTS

Figure 52